The Herbig Ae/Be stars associated with nebulosity (*)

U. Finkenzeller ([1]) and R. Mundt ([2])

([1]) Landessternwarte, Königstuhl, D-6900 Heidelberg 1, F.R.G.
([2]) Max-Planck-Institut für Astronomie, Königstuhl, D-6900 Heidelberg 1, F.R.G.

Summary. — We present a catalog of 57 Herbig Ae/Be stars and Herbig Ae/Be star candidates. For 43 of these objects, high resolution ($\Delta V = 18$ km/s) Hα and NaD line profiles have been obtained. We further have compiled all published optical and infrared magnitudes of these stars to study their variability, their infrared excesses and to calculate their luminosities. The major results are :

1. Most stars (50 %) have « double-peak » Hα line profiles separated by a nearly unshifted absorption component, while 25 % have « single-peak » Hα profiles, and 20 % have P Cygni profiles.

2. In no case has evidence for mass infall been found. The large Hα line widths are interpreted in terms of envelope expansion and rotation.

3. For the stars with P Cygni line profiles in Hα and NaD the following qualitative wind properties have been derived : their wind becomes accelerated within a few stellar radii; at larger distances (*e.g.* 20-50 R_*) the wind is nearly decelerated to its terminal wind velocity of 100-150 km/s; at these distances the wind is already cooled down below ≈ 5000 K by radiative cooling.

4. The photometric variation properties of early and late type Herbig Ae/Be stars are quite different. While most stars earlier than about B8-A0 show very small variations ($\Delta m_v < 0.05$ mag), the stars later than about B8 very often show large variation amplitudes ($0.5 \lesssim m_v \lesssim 2$ mag), which may be related to those of T Tauri stars.

5. The IR excesses of Herbig Ae/Be stars are much stronger than those of ordinary Be stars, and the two stellar groups are well separated in the *H-K*, *K-L* two-color diagram. Their IR excess cannot be explained by emission from a hot (10^4 K) ionized gas but is consistent with thermal emission from dust. The indicated dust temperatures are for most stars relatively high (1200-1500 K).

6. Stars later than B6 are generally located above the main sequence in the HR diagram which confirms that most of these stars are still in their pre-main-sequence stage of evolution. It is not regarded as tenable that their location in the HR diagram is due to rapid rotation, as suggested by Herbst *et al.* (1982).

Key words : Be stars — pre-main-sequence stars — stellar winds — emission lines — circumstellar shells — IR-excess — variability.

1. Introduction.

More than twenty years ago Herbig (1960) compiled a list of 26 Ae and Be stars suspected to be early type stars still in their pre-main sequence (PMS) stage of evolution. Herbig's selection criteria were :

(1) the spectral type is A or earlier, with emission lines,
(2) the star lies in an obscured region,
(3) the star illuminates fairly bright nebulosity in its immediate vicinity.

Herbig estimated that a considerable number of PMS stars earlier than A0 and brighter than $m_{pg} = 13$ should be observable within a distance of 1 kpc.

Detailed investigations by Strom *et al.* (1972) of about half of these 26 stars confirmed Herbig's suspicion of their PMS nature, since surface gravities and bolometric luminosities deduced for these objects placed them generally above the zero-age main sequence. In the meanwhile bolometric luminosities have been derived for a greater number of these objects. They are usually 1-2 mag higher than those of main sequence stars of the same spectral type (see *e.g.* Cohen, 1973b; Cohen and Kuhi, 1979).

The PMS nature of the Herbig Ae and Be stars (HBeS) has recently been questioned by Herbst *et al.* (1982). These authors suggested that the HBeS might be young stars on the main sequence, but rotating close to their break-up velocities.

In this study an effort is made to investigate various properties and aspects of these young stars in a broader context. For this purpose we compiled a list of 57 HBeS and HBeS candidates. For 43 of these stars we have obtained high resolution Hα and NaD line profiles. As we will see, these line profiles provide us, at least for some of the stars, with new insights in their stellar wind properties.

The stellar winds from these objects might have important consequences for the dynamics of the surrounding molecular cloud material, since several of these objects (LkHα 198, LkHα 208, R Mon, LkHα 234, V645 Cyg) are known from radio observations to be associated with high velocity molecular gas (Cantó *et al.*, 1981; Edwards and Snell, 1983; Bally and Lada, 1983). Furthermore the wind of R Mon very likely drives the proper motion of the Herbig-Haro (HH) object 39, located at the apex of the cone-like nebula NGC 2261 (Jones and Herbig, 1982). LkHα 234 has been suggested to be the exciting source for several HH objects in its vicinity (Cohen and Schwartz, 1983).

The study of an enlarged sample of HBeS was also motivated by the following question : which characteristics define unambiguously this class of very young stars ? The difficulty of finding unambiguous spectroscopic selection criteria for these young objects, *e.g.* comparable to those found for T Tauri stars, was already realized by Herbig (1960). As we will see, the line profiles obtained solve only part of this problem. We therefore tried to approach this problem from another side : with the help of literature data, we have investigated their photometric properties in the optical and infrared region, discussed variations, and compared them to related objects (*e.g.* Be and T Tauri stars). Especially the infrared data turned out to be a very useful tool in separating the HBeS from the classical Be stars, to which they are reminescent spectroscopically.

2. Selection of objects.

In table I, we have compiled a list of 57 stars which are HBeS and likely HBeS candidates. It is an updated version of an earlier list published by Finkenzeller (1982). In addition to Herbig's (1960) original list of 26 stars, table I contains stars from a variety of sources (see columns 6 and 8 of table I). We have tried to select only stars which follow Herbig's 1960 original definition (see Introduction). For this purpose we checked the appearance of each star on the Palomar Sky Survey prints to see whether they are located in an « obscured region » and whether they « illuminate fairly bright nebulosity in their immediate vicinity ». Nearly all emission line stars in table I fulfill these selection criteria. Early emission-line stars for which some selection criteria do not apply have been marked in table I by a « : » after the catalog number. These stars are still included in table I since we think they may be related to the other ones. We, in addition, marked all stars in table I with a « : » which turned out during the course of this study to have various peculiarities which make their membership to the HBeS doubtful (for details see Sect. 4).

As will be discussed later, the positions of the HBeS in an IR two-color diagram provides a further selection

criterion, especially for separating them from classical Be stars. For the present study we tried to obtain high resolution Hα and NaD line profiles of all stars in table I which were observable with the Steward Observatory 90 inch telescope echelle spectrograph. We were able to observe nearly all stars in table I which were north of about − 35 degrees and which were brighter than $V \approx 13$ mag. In total 43 stars were observed.

3. Observations and data reduction.

The spectra were obtained on 3 observing runs in 1981 using the cassegrain echelle spectrograph at the Steward Observatory 90 inch telescope (see table I for details on the dates and exposure times). This spectrograph uses photographic plates behind an RCA image tube (IIa-O plates baked in forming gas). With these plates about 18 echelle orders could be observed, giving a wavelength coverage of $\lambda\lambda 5700\text{-}7000$ Å. The projected slit width was usually 2 arcsec (or 60 μm at the plate), resulting in a resolution of about 16 km/s (or 0.35 Å at Hα) over the observed wavelength region. All plates were calibrated using a spot sensitometer (21 spots). For the wavelength calibration a Th-Ar hollow cathode lamp was utilized. Spectra of faint stars or of stars located in extended emission nebulosities ($\gtrsim 5$ arcsec) were not widened over the full slit length. Any possible contamination of the stellar spectrum by nebular emission or the sky spectrum (some plates were obtained during full moon) would thus be visible on the plates. The contribution of the night sky to the stellar continuum in no case exceeded 5 %, even for the plates with the longest exposure times. Therefore no corrections for night sky contaminations have been carried out. The emission lines from associated emission nebulae were in all cases considerably narrower than the stellar Hα emission and therefore are easily recognized in the Hα line profiles presented (see *e.g.* T Ori, or LHα 25 in Fig. 1). For these reasons no attempt has been made to correct the spectra for nebular contaminations.

The two orders containing Hα and the NaD were scanned with the Grant microdensitometer of the Max-Planck-Institut für Astronomie, Heidelberg. The tilt of the microdensitometer slit could (by a marginal amount) not be sufficiently adjusted to match the tilt of the lines in the individual orders, resulting in a slight decrease of resolution due to the registration process. From the FWHM of the comparison lines a resolution of 18 km/s (or 0.4 Å at Hα) could be measured. Intensity values were assigned by fitting an appropriately chosen polynomial to the density *vs.* log (I) table. Variations in the plate to plate background density were treated by subtracting the fog level before doing the fit.

In order to obtain a flat continuum the intensity tracings should be corrected for the echelle blaze response and the spatial sensitivity variations of the image tube. Ideally this should be done by a « flat field division ». Here we fitted the continua of the intensity tracings by a natural cubic spline, defined by at least 4 data points at suitable locations in the continuum. Subsequently we divided the intensity tracings by this continuum. This in general gave very satisfactory results. In some cases the Hα emission (or absorption) wing is rather broad and may therefore not have been recognized properly. However, this has

a small effect on the emission line profiles and the calculated Hα equivalent widths.

In figure 1 the Hα and NaD (with He I λ5876) line profiles of all 43 observed stars are displayed. For a few stars the echelle order with the NaD lines was located near the edge of the image tube cathode, resulting in a relatively poor S/N-ratio of the scans. The wavelength and velocity scale for all profiles in figure 1 is in the earth rest frame and was determined with the Th-Ar comparison lines. Any errors in this wavelength scale are expected to be smaller than about 0.6 Å (or 27 km/s at Hα). These errors and the fact that for half of the stars no heliocentric Hα velocities are available (see below) will not affect our conclusions drawn here.

Finkenzeller and Jankovics (1983) compared for about 10 stars the radial velocity of the interstellar NaD and Ca II H + K lines with the stellar radial velocity and that of the associated molecular cloud. Within their measurement errors ($\approx$ 5 km/s) they found no systematic velocity dispersion between the respective velocity values (see Herbig, 1977, in the case of T Tauri stars). Thus, the velocities of the interstellar NaD lines (*e.g.* in Fig. 2) provide us with an estimate of the stellar radial velocity.

Accurate heliocentric radial velocities of the Hα line profiles have been determined for a subsample of 25 stars. These are the objects for which more extensive line profile material on the higher Balmer lines exists. This material (together with the Hα radial velocities) will be discussed in a subsequent paper by Finkenzeller and Jankovics (1983). To obtain the heliocentric velocity values given in some of the profiles in figure 1 the appropriate area on each echelle plate was scanned with a PDS microphotometer. The IHAP image processing system of the ESO, Garching, was used for the subsequent rigorous treatment of image tilt and higher order dispersion effects. The internal error of the velocity values is about ± 3 km/s.

For all stars the total Hα equivalent widths (including the absorption components below the continuum) have been determined. The results are listed in table I. The main sources of error in Hα equivalent widths are uncertainties in the calibration curve, which are estimated to give a relative error of not more than 15 %, and the noise of the stellar continuum (resulting in an absolute error of about 0.5 Å). An independent control of the calibration procedure was made by using the ratio of equivalent widths of the [N II] λλ6548, 6584 lines present in some spectrograms. The nebular emission lines originate in an H II region in the vicinity of the respective star. The theoretical value of the EW ratio of the [N II] lines is 3.0 (Osterbrock, 1974). We measured a value of 3.1.

For comparison, profiles of 4 main sequence standard stars are also given at the end of figure 1. Due to the broad Hα absorption line wings systematic errors are possible (see above). The equivalent widths of the standards given in table I may therefore be slightly underestimated (as is the relative depth of the line profiles shown).

Eight stars of table I have in addition been studied with the Arizona/Smithsonian Multiple Mirror Telescope (MMT). An echelle spectrograph with a photon-counting Reticon was utilized to observe the echelle order covering the NaD lines and He I 5876. These MMT spectra are of higher resolution ($\Delta\lambda = 0.24$ Å, $\Delta v = 12$ km/s) and

higher S/N than the photographic echelle spectra obtained at the 90-inch telescope. For details on the data acquisition and reduction the reader is referred to Mundt and Hartmann (1983). The eight stars observed were BD + 61°154, V 380 Ori, HD 250550, R Mon, Z CMa, BD + 41°3731, BD + 46°3471, and MWC 1080. Their He I 5876 and NaD line profiles are displayed in figure 2, together with the observing dates. The heliocentric radial velocities of various circumstellar and interstellar absorption features in the NaD lines are indicated. The accuracy of these radial velocities is ± 2 km/s.

4. Comments on individual stars.

The Hα line profiles displayed in figure 1 have a large variety of shapes. We will classify and discuss the different types of profiles in more detail in the next section.

In most cases the NaD line profiles in figure 1 show the interstellar absorption components only. In about 25 % of the stars a weak, but mostly broad, NaD emission is observed, which in some cases shows P Cygni structure.

A visual inspection of all plates showed in about 30 % of the stars the presence of a mostly weak [O I] line, which could be easily distinguished from the corresponding night sky line by a much larger line width.

In about 25 % of the observed stars the He I λ5876 line appears in absorption and can be used for stars earlier than about B9 as an additional spectral type indicator. In a few cases the line appears in emission.

In table I, the general spectral characteristics of the stars are summarized. Beside others we list in table I the spectral type, the line profile type, the FWHM of Hα, the Hα equivalent width of the individual stars and whether [O I] λ6300, He I λ5876 and NaD is observed in emission (or absorption).

In the following we give comments on individual stars in order to point out interesting or peculiar spectroscopic properties. We compare our observations with previous work, and discuss the objects in view of their membership to the Herbig Ae/Be stars.

2. BD + 61°154: This star is long known from previous studies to show strong P Cygni absorption in many of its emission lines (see *e.g.* Herbig, 1960; Strom *et al.*, 1972). Velocity displacements of about − 400 km/s are evident in the Hα absorption component. The NaD and Hα line profiles given in figure 1 and 2 indicate variability. It should be mentioned that the Hα line profile of BD + 61°154 given by Garrison and Anderson (1977) had been interchanged with that of HD 200775 (for details see Köppen *et al.*, 1982). The large difference between the Hα equivalent widths of Garrison and Anderson (1977, 250 Å) and our work (34 and 55 Å) might not only be due to variations, but might be also due to overexposure mentioned by them. The sharp NaD absorption component visible in figure 2 at − 44 km/s is very probably of interstellar origin (see Münch, 1957, for observation of stars in this area).

3. XY Per A + B: A double star with a separation of about 2 arcsec. ($\Delta m = 2$ mag, aligned in *R.A.*). Our spectrogram contains the light from both components. The

central absorption dip in the Hα emission is practically unshifted.

5. **AB Aur**: A narrow (FWHM ≈ 80 km/s) P Cygni absorption component is evident at Hα($v \approx -250$ km/s). This feature is less conspicuous than in the Hα line profile of Garrison and Anderson (1977). Also the two Hα and NaD line profiles presented in figure 1 indicate variability. This is not unexpected, since AB Aur was noticed in previous investigations to be an active spectroscopic variable (*e.g.* Herbig, 1960). It is variable even on time scales of about one day (Praderie *et al.*, 1982). The line profile variations of this star on timescales of months to years have recently been studied by Finkenzeller (1983). The NaD lines appear as weak emissions. NaD line profiles of higher S/N have recently been obtained by Felenbok *et al.* (1983). In these profiles a weak blueshifted absorption is visible at -130 km/s. In our plate of January 18th, 1981, the weak emission feature at $\lambda 5872$ Å is due to scattered comparison light (a problem which occurred only in the spectra obtained in Jan. 1981).

6. **HK Ori**: The Hα emission line shows a weak self-reversal. A relatively broad red absorption wing is conspicuous in the NaD line profiles. Such a profile might be caused by a photospheric NaD absorption with the blue wing filled in by emission (however, only part of this emission could be due to the sharp NaD night sky emission components). Note that other absorption features typical of a late type star have been noticed (*e.g.*, Li I $\lambda 6707$ is present in our spectrogram or Ca II K in the spectra of Strom *et al.*, 1972). The presence of absorption features from both an early type star ($\approx$ A5) and a late type star ($\approx$ F5) has recently been confirmed by a detailed study of Davis *et al.* (1981). Therefore HK Ori might be a double star.

7. **BD + 9°880**: The blue wing of the Hα emission is considerably steeper than the red one, suggesting the presence of a stellar wind.

8. **T Ori**: This star is located in the Orion nebula region. Superimposed on the stellar spectrum are the narrow nebular emission lines of Hα and [N II] $\lambda\lambda 6543$, 6584. Notable is the redshift of the Hα absorption reversal of about 50 km/s with respect to the nebular Hα emission. The redshift of various (shell?) absorption features in the blue spectral range has already been noticed and discussed by Herbig (1960). The weak He I $\lambda 5876$ emission is of nebular origin.

9. **V380 Ori**: Both the Hα line and the NaD emission lines appear to be symmetric. Our measured Hα equivalent width is about half that of Garrison and Anderson (1977), indicating significant variability of this line. As in previous observations of this object (*e.g.* Herbig, 1960), numerous other broad emission lines are present on our echelle plate. In the high S/N-ratio spectrum shown in figure 2, the He I $\lambda 5876$ line appears in absorption ($W_\lambda \approx 0.1$ Å). The small width of this line indicates a $v \sin i$ value of about 30 km/s.

10. **BF Ori**: The star illuminates no nebulosity in its vicinity as is normally required to be identified as a HBeS. However, its IR-colors (see Table II and Fig. 4) are typical of HBeS.

11. **RR Tau**: The Hα line profile is similar to the one obtained by Garrison and Anderson (1977). However, in our spectrogram Hα has half the equivalent width as in the spectrogram of Garrison and Anderson (1977), suggesting significant variability.

12. **HD 37490**: A broad self-reversal is present in the Hα emission line. The width of the He I $\lambda 5876$ absorption line indicates a $v \sin i$ value in the order of 150 km/s. This star is in a reflection nebulosity and various patches of obscuration in the vicinity of this object are visible on the POSS prints. However this object has a weak IR excess and its K-L color is typical for classical Be stars (see table II and Vd). Therefore, its classification as a HBeS should be regarded as tentative.

13. **HD 250550**: A pronounced P Cygni profile is observed at Hα similar to the one published by Garrison and Anderson (1977) (see also Herbig, 1960; Strom *et al.*, 1972). The blue edge of the P Cygni absorption is at about -500 km/s. The NaD lines appear in emission as symmetric lines (with no indications of a stellar wind). Their widths (FWHM) is only half of the corresponding value of Hα. In the high S/N-ratio spectrum shown in figure 2 the He I $\lambda 5876$ absorption line possibly has a weak but broad emission component on its red side.

15. **MWC 137**: This star is unusual in several respects. It shows one of the strongest and broadest Hα emission lines of all observed stars. He I $\lambda 5876$ is a strong and broad emission line as well. The Hα, NaD and He I $\lambda 5876$ line profiles are very similar to those obtained by Ulrich and Knapp (1983). Many other allowed and forbidden lines are present on the echelle plate. It has been mentioned by Herbig and Rao (1972) that this object might not be a member of the Orion population. This is supported by its unusual line profiles. Furthermore MWC 137 is a strong radio emitter at 10 GHz. Its flux of 55 mJy (Walter, 1977) is much higher than that of any other HBeS observed so far (Bertout and Thum, 1982; Cohen *et al.*, 1982).

17. **HD 259431**: The Hα line profile is very similar to the one obtained by Garrison and Anderson (1977) with almost identical Hα equivalent widths. However, this star showed some variability about 50 years ago (Herbig, 1960). Variability has also been reported by Pogodin (1981). A He I $\lambda 5876$ absorption and a NaD emission line might be present.

20. **HD 52721**: This emission-line star is surrounded by a reflection nebula and it is located in a region of general obscuration as required for a HBeS. However, it has IR-colors and a (weak) IR-excess as a normal Be star (see table II and Vd), which makes its membership to the HBeS doubtful.

22. **Z CMa**: This star has very prominent and unusual P Cygni profiles in Hα and NaD. The blue edge of the P Cygni absorption extends to about -1000 km/s in Hα, whereas in the NaD lines the blue edge reaches only to about -500 km/s. In the NaD line profile in figure 2 several distinct velocity systems are indicated. Similar effects have been noted by Strom *et al.* (1972) for the H and He lines. Comparing the profiles in figures 1 and 2 with each other and with the profiles obtained by Ulrich and Knapp (1983), line profile variations are evident. Z CMa is a double star system of about 1.5 arcsec separation as could be seen with the slit viewing eye-pieces of various telescopes. The two components are aligned in

E-W direction and have about 10 mag and 12 mag, respectively.

24. HD 53367: This star might be a close binary system. This is supported by the following observations :

(1) The approximately symmetric Hα emission in figure 1 (from Nov. 14, 1981) is blueshifted by about − 75 km/s, while in a spectrum obtained 6 months earlier (May 15, 1981) the Hα line was highly redshifted to + 158 km/s. In another Hα line profile (from Dec. 9, 1981) it had a radial velocity of − 70 km/s (for details see Finkenzeller and Jankovics, 1983). Also noteworthy is the He I λ5876 line which shows a blueshifted emission peak ($v \approx -130$ km/s) and a roughly unshifted absorption component.

(2) Indications for radial velocity variations have been reported by Herbst and Assousa (1977) as well.

In contrast to most other stars discussed here this star has a very weak IR excess (see table II) and in the IR two-color diagram it is located among the classical Be stars (see Fig. 4 and Vd). This suggests that this star is likely to be a « normal » Be star in which the emission line activity may be due to its binary nature.

31. HR 5999: The Hα emission has a deep absorption reversal reaching well below the adjacent continuum. The line profile is variable in shape and intensity. Even stronger Hα line profile variations have been reported by Bessel and Eggen, 1972 (where the star is erroneously named HR 6000). The brightness and polarization variations of this star have been described by Thé *et al.* (1981, with further references therein). The star has relatively broad (FWHM $\approx$ 50 km/s) and strong NaD absorptions. According to Thé *et al.* (1981) the star is of spectral type A7 III. It is therefore plausible that the NaD absorptions are produced in the photosphere of the star. A strong and broad interstellar NaD absorption is very unlikely, if the star has only a distance of 270 pc and a foreground extinction of 0.2 mag as reported by Thé and Tjin A Djie (1978).

32. HD 150193: Hα has a P Cygni type profile with a sharp blue absorption at − 190 km/s. Weak emission might be present in the NaD lines.

34. KK Oph: Broad photospheric NaD absorptions are indicated suggesting a spectral type of about A5-A7.

35. HD 163296: Both the Hα line and the NaD lines have a pronounced P Cygni profile. The Hα line profile is slightly variable. No interstellar absorption component is detectable. This is unusual for a pre-main-sequence object which is supposed to be associated with molecular cloud material. Furthermore, no reflection (or emission) nebulosity is visible on the Palomar Sky Survey around this star, as it is the case with classical HBeS. This raises the question whether this is indeed a young object (which has somehow managed to move away from its parent molecular cloud) or whether it might be an evolved object leaving the main sequence. We note that this object has a strong IR excess as other HBeS (see table II) and in the IR two-color diagram in figure 4 it still falls in the distribution of other HBeS. However it is located at the far left side of the distribution with H-K = 0.73 and K-L = 0.9 (see also Vd).

36, 37. Lk Hα 118, 119: On both stellar Hα line profiles the strong, but narrow nebular emission from NGC 6523 (M8) is superimposed.

38. MWC 297: The Hα line ranks among the strongest ($W_\lambda(H\alpha) = 133$ Å) observed in our sample. The line is symmetric and has extended wings similar to MWC 137. A broad He I λ5876 absorption line seems to be present.

39. VV Ser: Comparing with the Hα and NaD line profiles of Ulrich and Knapp (1983) differences are evident. Unusual is the extended red absorption wing in the NaD line profiles (which is indicated in one of Ulrich's and Knapp's spectra as well). Similar NaD line profiles were observed in HK Ori. For HK Ori a possible interpretation appeared to be the superposition of blueshifted NaD emission on the broad photospheric NaD absorption. However, for VV Ser this interpretation can be excluded by the presence of a strong He I λ5876 line indicating a spectral type around B0-B3. A possible explanation might be cold descending material. The width of the He I λ5876 line indicates a $v \sin i$ value of 200 km/s.

40. MWC 300: The Hα profile is very similar to the one obtained by Ulrich and Knapp. Conspicuous are the extended wings of the Hα line as observed in other stars of our sample. Both the NaD lines and the He I λ5876 line show P Cygni structure. According to Herbig and Rao (1977) this object might not be a member of the Orion population (see also Allen and Swings, 1976). Furthermore this object is not associated with bright nebulosity.

41. AS 310: No (broad) stellar Hα emission is detectable. Therefore this object cannot be regarded as a Herbig Ae/Be star. With the slit viewing system of the coudé feed telescope at KPNO a companion star with a separation of 3 arcsec, $\Delta m \approx 1$ mag, and a position angle $\approx$ 135 deg. was seen.

42. TY CrA: The Hα absorption appears to be partially filled in by emission with a relatively sharp absorption at − 88 km/s. This profile is similar to the one described by Herbig and Rao (1972). Marraco and Rydgren (1981) also detected no Hα emission rising above the continuum.

43. R CrA, 44. T CrA: Herbig and Rao (1972) give a spectral type of F0 for these two stars which is too late to belong to the HBeS (limit : spectral type A). However their spectral type is not sufficiently well known to make a clear decision at the moment (*e.g.* Marraco and Rydgren, 1981, classify R CrA as A-type star).

45. BD + 40°4124: The Hα line profile is very similar to the one obtained by Garrison and Anderson (1977). However, we measured an equivalent width which is 30 % higher. A broad He I λ5876 line might be present.

46. BD + 41°3731: According to figure 1 and 2 a very broad and shallow He I λ5876 absorption might be present ($v \sin i \approx 400$ km/s). If the rotation of this star is indeed that high this explains (at least in part) the shallowness of the Hα absorption. No differences are indicated with respect to the profile obtained by Garrison and Anderson (1977). Herbig (1960) describes the star as having had « weak emission components... like an ordinary Be star in 1954 ». Due to the absence of (strong) Hα emission in our and Garrison's and Anderson's spectrogram the classification of this star as a HBeS should be regarded as very doubtful. This is furthermore supported by its IR colors (see

table II) which place this star in figure 4 among the classical Be stars (see also Vd).

49. HD 200775: This star had been interchanged by Garrison and Anderson (1977) with BD + 61°154. The correct profile agrees well with other observations (see also Finkenzeller, 1982; Baschek *et al.*, 1982; Köppen *et al.*, 1982). The widths of the He I λ5876 line indicates a $v \sin i$ value of about 70 km/s.

51. BD + 65°1637: The Hα line profile is very similar to the one measured by Garrison and Anderson (1977) and the measured equivalent width is identical to their value. A very broad and shallow He I λ5876 line seems to be present ($v \sin i \approx 300$ km/s).

52. Lk Hα 234: The general structure of the Hα line profile is similar to the profile published by Garrison and Anderson (1977). However, the blue part of the Hα emission in respect to the red emission peak is considerably weaker in our profile. Furthermore, we measured an equivalent width which is more than half as their value (25 Å *versus* 67 Å). P Cygni profiles at Hβ and Hγ have been reported by Strom *et al.* (1972). The presence of a stellar wind is indicated in Hα by the rather steep blue wing (of the strongest emission component). It is interesting that Edwards and Snell (1983) have found high velocity CO gas in the vicinity of Lk Hα 234 (and BD + 65°1637). Furthermore, several Herbig-Haro objects are in this area.

53. BD + 46°3471: Hα has a P Cygni profile with the absorption at about − 200 km/s. A P Cygni absorption seem to be present at the NaD lines as well ($v \approx -100$ km/s). Indications for a stellar wind in the NaD lines is provided also by the less extended blue wing than the red wing and by the steeper blue wing of these lines. The Hα profile differs significantly from the profile published by Garrison and Anderson (1977), while Ulrich and Knapp (1983) measured a similar line structure. Comparing figures 1 and 2, variability is indicated for the He I λ5876 line as well : in figure 2 a broad He I λ5876 absorption is clearly visible ($v \sin i \approx 250$ km/s), while there is no hint for any He I absorption in figure 1.

57. MWC 1080: Both the Hα line and the NaD lines show a pronounced P Cygni structure. Extended emission wings are present in Hα. The two strongest narrow NaD absorptions (at − 45 and − 15 km/s, see Fig. 2) are very probably of interstellar origin, as similar velocity components are observed in other stars in that area (Münch, 1957). The sharp weak component at − 72 km/s might be of interstellar origin as well. The general shape of the Hα profile does not differ from the one published by Garrison and Anderson (1977). However, in our spectrum the P Cygni absorption has only half the width than in their spectrum. Many other emission lines are visible on the echelle plate (see also Herbig, 1960).

5. Results and discussion.

5.1 STATISTICS, CORRELATIONS AND GENERAL PROPERTIES OF THE OBSERVED LINE PROFILES AND Hα EMISSION LINE STRENGTHS. — A large variety of line profiles and emission line strengths is observed in the Hα line, in the NaD and He I λ5876 line. Nevertheless, in over 90 % of all stars in

figure 1 the Hα line profiles can be roughly divided in the following three categories :

(*a*) single-peak profiles, consisting in many cases of a roughly symmetric emission line (abbreviated as Em. (s) in table I). Such profiles are observed in 25 % of all Hα emission stars.

(*b*) double-peak profiles, consisting of two emission peaks separated by an absorption reversal which is approximately unshifted in most cases (Em. (d) in table I). This type of profile is most common and was observed in 50 % of all emission line stars.

(*c*) P Cygni type profiles, having in most cases a blue absorption reaching below the adjacent continuum. In some cases emission is present on the blue side of the P Cygni absorption. P Cygni type profiles have been observed in about 20 % of all Hα emission stars (listed as P Cyg in table I).

A few objects (5 %) show more complex profiles and do not fit into this scheme (Em. (c) in table I).

In figure 3 we have plotted a histogram of the number of these three different line profile types as a function of spectral type. Figure 3 indicates that the double peak and P Cygni profiles are not distributed equally over the various spectral types. The double-peak profiles are more frequent among the stars earlier than A0, while the classifiable P Cygni profile stars are concentrated between B8 and A0.

The possibility of a dependence of the measured Hα equivalent widths on the spectral type was also considered. No correlation was found.

A comparison of the observed Hα line profiles with those of classical Be stars is of interest. Hα line profiles of similar resolution for Be stars have been published by Gray and Marlborough (1974, Δλ = 1 Å, 14 stars) and by Andrillat and Fehrenbach (1982, Δλ = 0.7 Å, 48 stars). In the latter study « double-peak » profiles are observed in 60 % of the investigated stars. « Single-Peak » profiles are observed in about 35 % of their stars. P Cygni profiles similar to those found among the HBeS are not observed in their sample. There are only a few stars representing about 5 % of the sample, which show indications for mass loss. These are the stars for which a steep blue emission edge, or a blueshifted Hα line center, or a weak blueshifted absorption dip is observed. Although selection effects for these two samples of stars cannot be excluded it is likely that the much larger number of stars with P Cygni profiles among the HBeS sample is significant.

5.2 STELLAR WIND PROPERTIES. — In many stars the half width of the Hα line at zero intensity exceeds 500 km/s. Although electron scattering might be important for the formation of the emission line wings, it is evident that in most of these stars mass motions of 300-500 km/s are present in the Hα emitting region. Since the HBeS are likely to be pre-main sequence stars one might consider that the observed velocities are due to the accretion of remnant star formation material (see *e.g.* Larson, 1969). However, in none of the Hα line profiles presented here, and in none of the line profiles of the higher Balmer lines (Finkenzeller and Jankovics, 1983) any evidence for mass accretion has been found (with the possible exception of VV Ser). As 20 % of

the observed stars show direct evidence for mass loss in the Hα line, we think that in general these mass motions are due to stellar winds. That in addition rotation might be important is suggested by the high $v \sin i$ values observed for some stars, and by the similarity of the double-peak line profiles to those observed in classical Be stars. In the latter stars such double-peak profiles have been interpreted by an envelope which is both rotating and expanding (Marlborough, 1969, 1970).

In the following we will discuss only the 8 stars with P Cygni type profiles at Hα. As we will see, some straightforward conclusions on their wind properties can be drawn. The 8 stars with P Cyg type profiles at Hα are BD + 61°154, AB Aur, HD 250550, Z CMa, HD 150193, HD 163296, BD + 46°3471, and MWC 1080. All but Z CMa (and may be HD 150193) have the NaD lines in emission. In 6 stars P Cygni absorptions are observed in NaD (see table III). In stars with single-peak and double-peak Hα profiles NaD emission are rare. This means NaD emission is a characteristic of the P Cygni stars and might be an indicator of high mass loss, as it seems to be the case for T Tauri stars (see Mundt, 1983).

In table II we compare the maximum negative velocity and the width of the NaD absorption with that of the Hα absorption for the stars with NaD and Hα P Cygni profiles. In general the blue edge of the NaD absorption is at less negative velocities than the blue edge of the Hα absorption and in most cases the width of the Hα absorption is larger than the corresponding NaD width.

A blueshifted NaD absorption is not expected to be formed very close to such early type stars (e.g. at a few R_*). Therefore the blueshifted NaD absorptions are probably formed at larger distances from the star (e.g. at 10-20 R_*) where sufficient neutral Na is present due to the cooling of the stellar wind ($T_e \lesssim 5000$ K). However, the blueshifted Hα absorption must be formed in wind regions which are sufficiently hot ($T \approx 10^4$ K) and dense to populate the $n = 2$ level by collisions. Therefore this region is very probably inside the relatively cold and more tenuous NaD absorption region. Combining these considerations with the results of table III the following wind properties are suggested if we assume spherical symmetry : the wind is accelerated to high velocities (≈ 400 km/s) in or below the formation region of the blueshifted Hα absorption, which is probably located a few stellar radii from the star (see also below). Further out (e.g. in the NaD absorption region) the wind is decelerated already by the gravitation of the star. In addition the wind is strongly cooled down by radiation cooling and by expansion as it reaches larger distances.

In the case of AB Aur, the observations of Finkenzeller (1983) indicate an even smaller size of the wind acceleration region than inferred from the above described line profiles : He has studied the profiles of the higher Balmer lines. For this purpose he has subtracted the spectrum of a B9 standard star from his AB Aur spectrum. The residual Balmer emission lines are highly asymmetric with their blue emission extending to about 400-600 km/s, while their red emission can be traced to about 250 km/s only. A similar, but even more conspicuous « blue-asymmetry » is observed in the He I λ5876 line of AB Aur in the high-quality spectrum obtained by Felenbok et al. (1983). This « blue-asymmetry » is likely to be caused by the occultation of the

receding part of an expanding and compact chromospheric region. In order to explain the observed line asymmetry quantitatively by occultation of spherical symmetric expanding chromosphere the emission line region of He I λ5876 and the higher Balmer lines must be smaller than $\approx 1.2\,R_*$. This means that the acceleration of the wind to velocities of about 400 km/s occurs in AB Aur at such small distances already. By similar occultation effects the Mg II λλ2795, 2802 line profiles of AB Aur can be explained qualitatively (Finkenzeller, 1983). It should be noted that similar conclusions on the velocity structure of the winds of 4 Herbig Ae/Be stars (including AB Aur) were drawn independently by Kuan and Kuhi (1975) from an analysis of the Balmer lines. Quite in contrast to the above conclusions Catala (1983) claims that AB Aur has an accelerating velocity field with small velocities (≈ 50 km/s) within a few R_* and a terminal velocity of 300 km/s. Catala's conclusions are mainly based on an analysis of the Mg II line profiles. However, such a velocity field is incompatible with the « blue-asymmetry » of the higher Balmer lines and the He I λ5876 line and the low velocity ($- 130$ km/s) of the narrow blueshifted NaD absorptions.

For the 6 stars with P Cygni absorptions at the NaD lines there is no emission beyond the blue edge of the absorption. This means that the NaD emission, like the blueshifted NaD absorption, is probably formed at relatively large distances from the star only with no contribution from the high-velocity regions close to the star. The same conclusions can probably be drawn for the 3 other P Cygni stars having pure NaD emission lines only. The lack of any high velocity NaD emission appears surprising, considering the fact that such emission could be formed by recombination in the dense, high velocity regions of the wind located close to the star. The absence of NaD emission from these regions might be due to the strong stellar radiation field. It could in principle ionize efficiently any Na atom recombined in an excited state and thus preventing its recombination to the ground state via the 4^2p level.

As the NaD emission in these stars is apparently formed outside the Hα emission, where the wind is already considerably decelerated (e.g. at about 10-20 R_*) the width of the NaD emission provides a mean to estimate (upper limits of the) terminal wind velocities. We have therefore measured the half width of the NaD emission at zero intensity. The results are summarized in the last column of table III. From these values we infer terminal wind velocities of 100-150 kms.

The mass loss rates of 4 stars discussed here have been determined by Kuan and Kuhi (1975) with the help of line profile calculations. For all 4 stars (BD + 61°154, AB Aur, HD 250550 and Z CMa) they obtained about the same mass loss rate of $\approx 2 \times 10^{-7}\,M_\odot$/yr. Although it is difficult to estimate the accuracy of such determinations it is likely that they are order of magnitude estimates only. Therefore new line profile calculations including our NaD line profiles and other recently obtained line profile data would be desirable (e.g. Finkenzeller and Jankovics, 1983).

The wind properties of the HBeS with P Cygni profiles at Hα seem to be similar to those of high-mass-loss T Tauri stars (see Mundt, 1983). The observations of Mundt suggest that their winds are decelerated at larger distances

from the star also. The terminal wind velocities estimated for some of the observed T Tauri stars are 100-150 km/s, which is close to the values derived above. As in the HBeS the more distant regions of the T Tauri star winds are relatively cool as indicated by various blueshifted absorption features found in the NaD lines or in the Ca II H and K lines.

A possible driving mechanism for the winds in T Tauri stars are Alfvén waves (*e.g.* Hartmann *et al.*, 1982). Could Alfvén waves also drive the stellar winds in the HBeS discussed here ? Due to the similarities with T Tauri star winds and due to the difficulties with a radiatively driven wind (Kuan and Kuhi, 1975) we regard this a worthwhile consideration. One might object against this hypothesis that such early type stars ($\approx$ A0) are not at all expected to have convection zones which are necessary to generate variable magnetic fields in their atmospheres.

For these aspects Bastian (1982) made an interesting suggestion. He argues that in very young stars convection zones may occur at earlier spectral types than is usually expected : during the main accretion phase in the Larson (1969) model of star formation, stars with moderate masses are strongly heated from outside by the accretion shock. Therefore fairly hot layers are present not far below the star's surface when the heavy mass accretion ceases. In the subsequent phase when the star begins to adjust its interior towards a main-sequence structure, very steep temperature gradients may occur close to the surface. This mechanism might trigger convection even without a hydrogen ionization zone.

In our sample P Cygni line profiles are observed in stars with a spectral of B8-A0. In the above picture this would mean that the onset of convection is shifted to a spectral type of about B8 in recently formed stars, as compared to a convection limit at early F on the main sequence. Although these considerations are very speculative, we think that they deserve future investigations.

5.3 PHOTOMETRIC AND SPECTROSCOPIC VARIABILITY. — Several HBeS have been long known as variables (Herbig, 1960). From the 57 stars in table I, 15 are listed in the General Catalog of Variable Stars (Kukarkin, 1969) and 3 additional stars (HD 37490, CoD − 44°3318, BD + 46°3471) are found as suspected variables. The range in photographic magnitude of these variables is given in table I. Typical values are 2 mag but can reach in a few cases up to 4 mag.

Whether all HBeS are variable and on what level is an interesting question. The relatively small fraction ($\approx$ 25 %) of known variables in table I indicates already that not all of them can be strong photometric variables. We have investigated the photometric variation amplitudes of the HBeS by collecting all photoelectric UBV measurements available in the literature. For 22 stars measurements in at least 2 nights are available (see table II). About 50 % of these stars showed no variations larger than about 0.05 mag, which is quite small compared to the large variation amplitudes of some HBeS. This discrepancy becomes understandable if one investigates the number of variable stars and the variation amplitudes as a function of spectral type, which has been done in figure 4. As evident from this figure nearly all strongly variable stars

(93 %) have spectral types *later* than B8 and all stars with no significant variations ($\lesssim$ 0.05 mag) have spectral types *earlier* than A0. This means that between spectral type B8 and A0 a radical change in the variation behavior occurs, with stars later than B8 being on the average much stronger variable. The variation amplitudes of the latter stars are similar to those of T Tauri stars (Herbig and Rao, 1972). It is therefore conceivable that similar mechanisms cause the variations in both the T Tauri stars and the late type HBeS (*e.g.* magnetically active regions on the stellar surface). Maybe the larger variation amplitude for stars later than B8-A0 mark the onset of convection in these stars (see also above).

The small photometric variability of the early type HBeS seems to be more similar to that of the classical Be stars. Feinstein (1968), for example, observed for only half of his 72 investigated Be stars small variations (0.06-0.1 mag) and very few stars had larger variation amplitudes (up to 0.3 mag).

In table IV we have compiled all $W_\lambda(H\alpha)$ values of HBeS available in the literature to get some ideas about the variability in this line (typical errors of $W_\lambda(H\alpha)$ 10-20 %). As evident from this table significant variations in Hα occur among the early type HBeS as well (*e.g.* LkHα 220, BD + 40°4124, BD + 65°1634, LkHα 234). For two of these four stars line profile variations have been observed, as has been described in section 4.

5.4 IR EXCESS AND *H-K, K-L* TWO-COLOR DIAGRAM. — The IR excess of HBeS and related young stellar objects is generally interpreted by thermal emission from hot, circumstellar dust (Strom *et al.*, 1972 ; Cohen, 1973b ; Cohen and Kuhi, 1979 ; Rydgren and Vrba, 1982). An alternative mechanism which might be applicable to some HBeS is Bremsstrahlung of H_2^- from a relatively cold ($T = 2000$-3000 K) and extended region ($R = 50$-100 R_*) around these stars (Lorenzetti *et al.*, 1982).

In the following we will discuss the infrared properties of HBeS in the context of thermal dust emission. This interpretation is favored here for the following reasons : (1) All HBeS are located in reflection nebulae, which implies that at least at larger distances from these stars dust is present. (2) Their relatively high intrinsic polarisation is an indication of stellar light scattered at circumstellar or nebular dust (Vrba *et al.*, 1979). Especially the polarisation variability of some stars on 1 year time scales indicates that the scattering dust must be relatively close to the star (*e.g.* 1 AU, if we assume that the variability is due to dust clumps moving in Keplerian orbits). (3) A 10 μ silicate emission has been observed in the IR spectrum of V 380 Ori and AB Aur (Cohen, 1973a), and in HD 97048, Elias 1, and in TY CrA the dust related emission features at 3.3 μ (or 3.4 μ and 3.5 μ) have been detected (Whittet *et al.*, 1983). (4) The IR colors of all HBeS with strong IR excesses are consistent with thermal emission from dust (see below), whereas alternative IR emission mechanisms are not applicable to all stars (Cohen, 1973b ; Cohen and Kuhi, 1979 ; Lorenzetti *et al.*, 1983).

In table II we have compiled the *H, K, L, M* data of all HBeS for which such data are available in the literature. If possible, we have given preference to those data for

which the observations have been carried out (quasi) simultaneously. In table II we give A_V values and IR excesses at $L (= 3.5 \mu)$ as well. The A_V values have been derived with $R = 3.1$ from the B-V colors given in table II assuming intrinsic colors of a main sequence star with the same spectral type as given in table I (intrinsic colors from Schmidt-Kaler, 1982). The IR excesses at 3.5 μ has been defined by $(V-L) - (V-L)_0$, where V-L is the dereddened measured color and $(V-L)_0$ is the intrinsic color of a main sequence star with the same spectral type (Johnson, 1966). The typical values for the IR excess are 3-5 mag. We have searched for correlations between the IR excess and the equivalent width of $H\alpha$, the $H\alpha$ line profile type and the spectral type. No correlation was found. The lack of any correlation between the IR excess emission and the $H\alpha$ emission strongly suggests that both types of emission are not formed in the same region (e.g. in a 10^4 K gaseous envelope). This is further indicated by the location of the HBeS in the IR two color diagram (see below).

In figure 5 we have placed all stars with known H, K, L values in a dereddened H-K, K-L two-color diagram. We have dereddened their measured colors with the A_V values from table II ($A_V : A_H : A_K : A_L = 1 : 0.2 : 0.12 : 0.06$). For stars with poor spectral types, for which no A_V values are given in table II, we have assumed intrinsic colors of an A0 star. Although errors in A_V of about 1 mag are possible for such stars, these errors have small effects on the location of these stars in the H-K, K-L diagram. For comparison with the HBeS we have plotted in figure 5 a number of classical Be stars also (data from Allen, 1973, and Jaschek et al., 1981). As evident form figure 5 the HBeS have rather different IR colors than the classical Be stars and the two groups of stars are well separated in this diagram. Most HBeS (85 %) in figure 5 have H-$K > 0.4$ and K-$L > 0.8$, while the classical Be stars have H-$K < 0.2$ and K-$L < 0.5$. This means that large IR colors provide an excellent criterion to separate HBeS from normal Be stars. The few HBeS with colors similar to Be stars are HD 37490 (# 12), HD 52721 (# 20), HD 53367 (# 24), TY CrA (# 42), BD 41°3731 (# 45), and BD 65°1637 (# 51). Three of these stars show spectroscopic pecularities (see Sect. 4) : HD 53367 is probably a spectroscopic binary which might explain its emission line spectrum, while TY CrA and BD + 41°3731 showed no $H\alpha$ emission above the continuum in our spectra which makes their HBeS membership doubtful, anyway. The other three stars fulfill all of Herbig's original selection criteria, but their IR colors indicate that they may be normal Be stars being (accidentally ?) associated with dark cloud material.

In figure 5 we have indicated by a square the locus of the free-free, free-bound and bound-bound emission from an optically thin hydrogen gas with an electron temperature of 10^4 K (Cohen and Kuhi, 1979). Most HBeS are located to the right of that square. Thus, the IR excesses of most HBeS cannot be explained by the emission from a 10^4 K hydrogen gas, which is also indicated by the lack of any correlation between IR excess emission and $H\alpha$ emission. The IR colors are, however, consistent with the thermal emission from dust, as can be demonstrated by a series of curves plotted in figure 5. These curves correspond to an A0 star photosphere with increasing amounts

of superimposed thermal emission from hot dust (800-1500 K). Dust temperatures between 700-1500 K are indicated. A large fraction of stars have dust temperatures of 1200-1500 K. However, some of the high dust temperature values might be due to unreliable IR colors and A_V values.

Interestingly, high dust temperatures ($T \approx 1300$ K) have been observed in many T Tauri stars as well (Rydgren and Vrba, 1982). For both types of objects the high dust temperatures imply small distances from the star (e.g. 20-50 R_*). This raises the question as to whether this can still be dust from the parent molecular cloud considering the strong stellar winds all these stars might have, or if this can be dust formed in the stellar wind of these objects.

5.5 BOLOMETRIC LUMINOSITIES AND HERTZSPRUNG-RUSSELL DIAGRAM. — Continuous energy distributions for all stars were constructed by combining the measured optical 0.35 μ and 0.55 μ fluxes with the 1-5 μ IR fluxes. If available in the literature (e.g. from Cohen, 1973a) fluxes at longer wavelengths (up to 20 μ) have been considered as well. The fluxes were extrapolated to infinite wavelength using the method of Cohen (1973b). Since for most stars we do not know whether the observed extinction is mainly circumstellar or interstellar we have estimated the bolometric luminosity from these fluxes in two ways. One way is by assuming that all extinction is circumstellar and the other by assuming that the extinction is mainly interstellar. We will designate the luminosities calculated with these two assumptions L_{min} and L_{max}, respectively.

L_{min} is calculated by integrating over the measured energy curve without applying reddening corrections, while for the calculation of L_{max} the energy curve has been corrected for extinction ($A_U : A_B : A_V : A_J : A_H : A_K : A_L : A_M = 1.56 : 1.3 : 1 : 0.3 : 0.2 : 0.12 : 0.06 : 0.04$). Thus, L_{min} represents a lower limit of the actual stellar luminosity. However, if the interstellar extinction can be ignored and if the circumstellar extinction is strong enough ($A_V \gtrsim 1$) to absorb all UV photons with $\lambda \lesssim 0.35 \mu$ and to redistribute their energy to IR wavelengths via thermal dust emission, L_{min} is not merely a lower limit but represents a reasonable estimate of the true stellar luminosity. In order to regard L_{max} as an upper limit of the stellar luminosity the implicit assumption is made that all UV photons are transformed into IR photons. Depending on the dust properties a circumstellar extinction of $A_V = 0.5$ at 0.5 μ might be already sufficient to absorb most photons in the UV, where the hot HBeS emit the bulk of their energy. However, if not all of the UV flux is redistributed both L_{min} and L_{max} will underestimate the actual values. All the conclusions drawn in this chapter are independent of this remaining uncertainty. L_{min} and L_{max} are listed in table II together with the distances used for their calculation. These distances are from various literature sources (beside others from Strom et al., 1972; Cohen, 1973b; Cohen and Kuhi, 1979; Herbst et al., 1982a). The assumption of spherical symmetry has implicitly been used for the calculation of L. However, this assumption is only wrong in cases like an edge-on or pole-on disc and is not expected to cause systematically wrong luminosities.

In figure 6 we present a Hertzsprung-Russell (HR)

diagram for the HBeS. This figure contains all stars with known L_{min} and L_{max} and with sufficiently well known spectral types, *i.e.* stars for which we think the spectral type is more accurate than 3-4 subclasses. In general we expect an accuracy of 1-2 subclasses (or 0.03-0.05 in $\log T_{eff}$) as derived by comparing the spectral types given by various literature sources. The spectral types have been transformed into effective temperature with the same relations used by Cohen and Kuhi (1979), which assume that these stars have similar temperatures as main sequence stars. In figure 6 we have plotted L_{min} and L_{max}. As evidenced in this figure most L_{min} values for $\log T_{eff} < 4.1$ (or later than B6) are located above the main sequence. For earlier stars this is not the case; even the L_{max} values are close to the main sequence. As discussed above this does not imply luminosities similar to main sequence stars, since L_{max} is not a true upper limit of the luminosity. However, it is interesting that 3 of the 5 stars with $\log T_{eff} > 4.2$ have small IR excesses (similar to normal Be stars).

The location of these stars above the main sequence together with several other arguments, like their close association with molecular cloud material, strongly indicates their pre-main sequence (PMS) nature (Strom *et al.*, 1972). This interpretation has recently been questioned by Herbst *et al.* (1982) who suggested that HBeS are ordinary Be stars associated with dark cloud material, rather than being PMS objects. The location above the main sequence is interpreted by rapid rotation, an effect which seems to explain the shift of normal Be stars above the main sequence (Collins and Sonneborn, 1977). As discussed by the latter authors this effect is highly nonlinear and requires rotation very close to the break-up velocity ω_C to cause any significant shifts in the HR diagram. For the normal Be stars 0.9 ω_C is required to explain their location in the HR diagram. A rotation of 0.9 ω_C causes mainly a temperature decrease of ≈ 0.08 in $\log T$ at 10^4 K (Collins and Sonneborn, 1977). Thus, by a rotation similar to ordinary Be stars the HR diagram location of most HBeS ($\approx 70\%$) cannot be explained. One would really require a rotation at ω_C to explain most HBeS, which results in a further decrease in $\log T$ by ≈ 0.1. The rotational velocities of a sample of 17 HBeS have recently been discussed by Davis *et al.* (1983). They showed that stars of spectral type B6-B9 ($\log T = 4.15$-4.04) rotate significantly slower than ordinary Be stars. Only HBeS of earlier spectral type may have similar rotational velocities. Due to these observations and due to the above considerations we regard the suggestion of Herbst *et al.* (1982) no longer tenable for HBeS later than B6.

References

ALLEN, D. A. : 1973, *Mon. Not. R. Astron. Soc.* **161**, 145.
ALLEN, D. A., SWINGS, J. P. : 1976, *Astron. Astrophys.* **47**, 293.
ANDRILLAT, Y., FEHRENBACH, Ch. : 1982, *Astron. Astrophys. Suppl. Ser.* **48**, 93.
BALLY, J., LADA, C. J. : 1983, *Astrophys. J.* **265**, 824.
BASCHEK, B., BELTRAMETTI, M., KÖPPEN, J., TRAVING, G. : 1982, *Astron. Astrophys.* **105**, 300.
BASTIAN, U. : 1982, private communication.
BERTOUT, C., THUM, C. : 1982, *Astron. Astrophys.* **107**, 368.
BESSEL, M. S., EGGEN, O. J. : 1972, *Astrophys. J.* **177**, 209.
CANTÓ, J., RODRÍGUEZ, L. F., BARRAL, J. F., CARRAL, P. : 1981, *Astrophys. J.* **244**, 102.
CATALA, C. : 1983, Thesis, Université de Paris VII.
COHEN, M. : 1973a, *Mon. Not. R. Astron. Soc.* **161**, 105.
COHEN, M., BIEGING, J. H., SCHWARTZ, P. R. : 1982, *Astrophys. J.* **253**, 707.
COHEN, M., KUHI, L. V. : 1979, *Astrophys. J. Suppl. Ser.* **41**, 743.
COHEN, M., SCHWARTZ, R. D. : 1983, *Astrophys. J.* **265**, 877.
COLLINS, G. W., SONNEBORN, G. H. : 1977, *Astrophys. J. Suppl. Ser.* **41**, 734.
DAVIS, R., STROM, S. E., STROM, K. M. : 1981, *BAAS* **13**, 855.
DAVIS, R., STROM, S. E., STROM, K. M. : 1983, *Astron. J.* **88**, 1644.
DIBAI, E. A. : 1969, *Astrofizika* **5**, N° 2, 249.
EDWARDS, S., SNELL, R. L., 1983, *Astrophys. J.* **270**, 605.
FEINSTEIN, A. : 1968, *Z. Astrophys.* **68**, 29.
FELENBOK, P., PRADERIE, F., TALAVERA, A. : 1983, *Astron. Astrophys.*, submitted.
FINKENZELLER, U. : 1982, *Be stars*, IAU Symposium N° 98 (eds. M. Jaschek and H.-G. Groth).
FINKENZELLER, U. : 1983, *Astron. Astrophys.* **124**, 157.
FINKENZELLER, U., JANKOVICS, I. : 1983, *Astron. Astrophys.*, submitted.
GARRISON, L. M., ANDERSON, C. M. : 1977, *Astrophys. J.* **218**, 438.

GRAY, D. F., MARLBOROUGH, J. M. : 1974, *Astrophys. J. Suppl. Ser.* **27**, 121.
HARTMANN, L., AVRETT, E. M., EDWARDS, S. : 1982, *Astrophys. J.* **261**, 279.
HERBIG, G. H. : 1960, *Astrophys. J. Suppl. Ser.* **4**, 337.
HERBIG, G. H. : 1977, *Astrophys. J.* **214**, 747.
HERBIG, G. H., RAO, N. K. : 1972, *Astrophys. J.* **174**, 401.
HERBST, W., ASSOUSA, G. E. : 1977, *Astrophys. J.* **217**, 473.
HERBST, W., MILLER, D. E., WARNER, J. W., HERZOG, A. : 1982, *Astron. J.* **87**, 98.
IBEN, I. : 1965, *Astrophys. J.* **142**, 993.
JASCHEK, M., HUBERT-DEPLACE, A.-M., HUBERT, H., JASCHEK, C. : 1981, *Astron. Astrophys. Suppl. Ser.* **42**, 103.
JOHNSON, H. L. : 1966, *Ann. Rev. Astron. Astrophys.* **4**, 193.
JONES, B. F., HERBIG, G. H. : 1982, *Astron. J.* **87**, 1223.
KUAN, P., KUHI, L. V. : 1975, *Astrophys. J.* **199**, 148.
KUKARKIN, B. V. : 1969, *General Catalog of Variable Stars,* Moscow.
KÖPPEN, J., BELTRAMETTI, M., FINKENZELLER, U., MUNDT, R. : 1982, *Astron. Astrophys.* **112**, 174.
LARSON, R. B. : 1969, *Mon. Not. R. Astron. Soc.* **145**, 211.
LORENZETTI, D., SARACENO, P., STRAFELLA, F. : 1983, *Astrophys. J.* **264**, 554.
MARLBOROUGH, J. M. : 1969, *Astrophys. J.* **156**, 135.
MARLBOROUGH, J. M. : 1970, *Astrophys. J.* **159**, 575.
MARRACO, H. G., RYDGREN, A. E. : 1981, *Astron. J.* **86**, 62.
MÜNCH, G. : 1957, *Astrophys. J.* **125**, 42.
MUNDT, R., HARTMANN, L. : 1983, *Astrophys. J.* **269**.
MUNDT, R. : 1983, *Astrophys. J.,* in press.
OSTERBROK, D. E. : 1974, in « *Astrophysics of Gaseous Nebulae* » (Freeman and Co., San Francisco).
POGODIN, M. A. : 1981, *Astron. Zh.* **58**, 796.
PRADERIE, F., TALAVERA, A., FELENBOK, P., CZARNY, J., BOESGAARD, A. M. : 1982, *Astrophys. J.* **254**, 658.
RYDGREN, A. E., VRBA, F. J. : 1982, *Astrophys. J.* **256**, 168.
SCHMIDT-KALER, T. : 1982, *Landolt-Börnstein,* **VI** 2, 14.
STROM, S. E., STROM, K. M., YOST, J., CARRASCO, L., GRASDALEN, G. : 1972, *Astrophys. J.* **173**, 353.
THÉ, P. S. *et al.* : 1981, *Astron. Astrophys. Suppl. Ser.* **44**, 451.
THÉ, P. S., TJEN A DJIE, H. R. E. : 1978, *Astron. Astrophys.* **62**, 439.
ULRICH, R., KNAPP, G. R. : 1983, in preparation.
VRBA, F. J., SCHMIDT, G. D., HINTZEN, P. M. : 1979, *Astrophys. J.* **227**, 185.
WALTER, H. G. : 1977, *Astron. Astrophys. Suppl. Ser.* **30**, 381.
WHITTET, D. C. B., WILLIAMS, P. M., BODE, M. F., DAVIES, J. K., ZEALEY, W. J. : 1983, *Astron. Astrophys.* **123**, 301.

Description of table I

[1] Catalog number, increasing with *R.A.*
[2] Star designation. Objects which may not definitely belong to the class of Herbig Ae/Be stars are marked with a colon (:).
[3] Right Ascension (*R.A.*) at equinox 1900.0.
[4] Declination (*Delta*) at equinox 1900.0.
[5] Photographic magnitude.
[6] Reference of the photographic magnitude.
[7] Spectral type.
[8] Reference of the spectral type.
[9] Hα equivalent width [Ångströms]. Emission is indicated by a negative sign.
[10] For Hα the full width at half maximum (FWHM) of the emission is given [km/s].
[11] For the profile types the following abbreviations are used :
 — « Abs. » is indicating a photospheric absorption feature.
 — « PCyg » indicates a P Cygni type profile.
 — « Em. (s) » stands for a single-peak emission line.
 — « Em. (d) » is indicative of a double-peak emission normally separated by a self-reversal.
 — « Em. (c) » denotes complex emission profiles.
[12] The presence of the stellar nebular line 0[I] $\lambda6300$ is indicated by a cross (X).
[13] The presence of the sodium D lines in emission is indicated by a cross (X).
[14] The presence of HeI $\lambda5876$, if any, in emission or absorption is given.
[15] Steward Observatory plate number.
[16] UT date of observation.
[17] Exposure time [minutes].

Description of table II

[1] Catalog number, increasing with *R.A.*
[2] Star designation. Objects which may not belong to the class of Herbig Ae/Be stars are marked with a colon (:).
[3] Arithmetic mean of available *V* magnitudes.
[4] Total range of variations in *V*.
[5] Number of nights used to derive ΔV.
[6] Arithmetic mean of available *U-B* values.
[7] Arithmetic mean of available *B-V* values.
[8] References for [3]-[7].
[9]-[13] Infrared data, if available.
[14] References to [9]-[13].
[15] Visual extinction Av, calculated with $R = 3.2$, (*B-V*) from [7] and assuming intrinsic (*B-V*) colors of a main sequence star with the spectral type given in table I.
[16] Infrared excess at *L*, definition see text.
[17] Bolometric luminosity, calculated by integrating the observed flux without applying reddening corrections.
[18] Bolometric luminosity after applying the standard reddening corrections.
[19] Distances adopted for the determination of the luminosities. Sources see text.

TABLE I. — *Catalog of Herbig Ae/Be stars and observing log.*

[1] #	[2] Star	[3] R.A. (1900)	[4] Delta (1900)	[5] m(pg)	[6] Ref.	[7] Spectral Type	[8] Ref.	[9] $W_\lambda H\alpha$ [Å]	[10] $H\alpha$ FWHM [km/s]	[11] $H\alpha$ Profile Type	[12] [OI] stel.	[13] NaD Em.	[14] HeI 5876	[15] S.O. Plate	[16] UT Date	[17] Exp. [min]
1	Lk Hα198	0h06.1m	+58 17′	15	(1)	A:ep	(6)									
2	BD +61°154	0 37.5	+61 22	10.6	(1)	B8-B9eq	(22)	-34	250	PCyg		X	Abs.:	198	22-May-81	23
								-55	180					289	18-Nov-81	36
3	XY Per A+B	3 42.9	+38 40	9.2-10.6	(3)	A2II+B6e	(17)	- 6	400	Em.(d)	X:			290	18-Nov-81	16
4	Elias 1	4 12.5	+28 04	15	(4)	A0:	(4)									
5	AB Aur	4 49.4	+30 23	7.2-8.4	(1)	B9e	(6)	-22	240	PCyg		X		140	18-Jan-81	8
								-27	250					255	14-Nov-81	5
6	HK Ori	5 25.9	+12 05	11.1-13.3	(1)	A4ep	(6)	-45	250	Em.(d)	X			292	18-Nov-81	71
7	BD +9°880	5 29.2	+9 58	9.3	(5)	A5e	(5)	-12	180	Em.(s,c)				256	14-Nov-81	19
8	T Ori	5 30.9	- 5 32	9.5-12.6	(1)	A3e	(6)	- 9	280	Em.(d)	X			266	15-Nov-81	42
9	V380 Ori	5 31.6	- 6 47	9.7-10.3	(1)	A1e	(6)	-58	260	Em.(s)		X		277	16-Nov-81	25
10	BF Ori	5 32.4	- 6 39	9.8-13.4	(6)	A-Fpe	(6)	-13	350	Em.(d)				267	14-Nov-81	74
11	RR Tau	5 33.3	+26 19	10.2-14.2	(1)	A3-A5e	(22)	-50	260	Em.(d)	X			276	14-Nov-81	84
12	HD 37490	5 33.9	+ 4 04	4.4	(2)	B3IIIe	(17)	- 6	350	Em.(d)			Abs.	254	14-Nov-81	6
13	HD 250550	5 56.2	+16 31	9.7	(1)	B9eq	(6)	-48	220	PCyg		X		294	18-Nov-81	9
14	Lk Hα208	6 02.1	+18 42	13.0	(1)	B5-B9e	(6)	- 5	210	Em.(d)				278	16-Nov-81	54
15	MWC 137	6 13.0	+15 19	11.2	(6)	cont+e	(6)	-133	300	Em.(s)	X	Em.		282	16-Nov-81	70
16	Lk Hα215	6 27.2	+10 14	10.5	(1)	B7-B8e	(22)	-17	380	Em.(d)				280	16-Nov-81	30
17	HD 259431	6 27.6	+10 24	8.7	(1)	B6pe	(1)	-52	200	Em.(d)	X	X:	Abs.:	279	16-Nov-81	8
18	R Mon	6 33.7	+ 8 50	11.3-13.8	(1)	e+s	(1)									
19	L Hα25	6 35.2	+ 9 53	13.0	(1)	B8pe	(6)	-44	340	Em.(d)	X			295	18-Nov-81	70
20	HD 52721	6 57.2	-11 09	6.40	(2)	B2Ve	(19)	- 4	320	Em.(s)	X	Abs.		288	14-Nov-81	6
21	Lk Hα218	6 58.0	-11 17	12.2	(7)	B6e	(7)	-19	300	Em.(d)				269	15-Nov-81	68
22	Z CMa	6 59.0	-11 24	8.8-11.2	(1)	eq	(6)	+ 1	100	PCyg				283	16-Nov-81	14
23	Lk Hα220	6 59.6	-11 18	12.3	(7)	B5e	(7)	-35	280	Em.(s)			Abs.	268	15-Nov-81	67
24	HD 53367	6 59.7	-10 18	7.0	(1)	B0IV:e	(1)	-11	270	Em.(s)			Em./Abs.	260	14-Nov-81	13
25	CoD -44°3318	7 16.4	-44 24	10.4	(20)	A-Fe	(23)			Em.(d)						
26	HD 76534	8 51.5	-43 05	7.5	(2)	B3e	(17)			Em.(d)						
27	RCW 34	8 52.6	-42 44	11	(2)											
28	RCW 36	8 55.7	-43 21	11	(2)											
29	Herbst 28	8 54.8	-43 03	11.5	(2)	B5Ve	(2)									
30	HD 97048	11 05.3	-77 07	8.4	(6)	A0e	(20)			PCyg						
31	HR 5999	16 01.9	-38 50	6.4	(9)	A7III-IVe	(9)	- 6	450	Em.(d)	X:			194	22-May-81	12
								- 9	420					215	18-Jun-81	8
								- 5	400					231	14-Jul-81	20
32	HD 150193	16 34.4	-23 42	8.6	(4)	A0e	(18)	- 5	140	PCyg		X:		193	22-May-81	25
33	CoD -42°11721	16 52.0	-42 33	11	(10)	Be	(10)									
34	KK Oph	17 03.9	-27 08	11.8-12.7	(6)	A5-A7e	(23)	-17	310	Em.(d)	X			189	21-May-81	65
35	HD 163296	17 50.3	-21 56	6.8	(11)	A0Ve	(18)	-12	190	PCyg		X		184	20-May-81	6
								-17	190					199	23-May-81	18
36	Lk Hα118	17 59.7	-24 16	12	(6)	B5Vpe	(12)	-18	400	Em.(s)	X			203	16-Jun-81	46
37	Lk Hα119	18 00.1	-24 18	13	(12)	B1Ve	(12)	-14	280	Em.(s)	X			209	17-Jun-81	80
38	MWC 297	18 22.4	- 3 55	11.0	(1)	?	(1)	-133	380	Em.(s)	X	X:	Abs.:	201	16-Jun-81	58
39	VV Ser	18 23.7	+00 05	11.4-12.7	(6)	B1-B3e:	(23)	-22	330	Em.(s)	X	X:	Abs.	208	17-Jun-81	82
40	MWC 300	18 24.1	- 6 09	12.5	(6)	eq	(6)	-78	120	Em.(d)	X	X	PCyg	214	18-Jun-81	74
41	AS 310	18 28.0	- 5 03	10	(6)	B-Ae	(6)							195	22-May-81	48
42	TY CrA	18 54.9	-37 01	8.7-12.4	(6)	B9(e)	(6)	+ 2		Abs.				204	16-Jun-81	27
43	R CrA	18 55.1	-37 06	10.0-13.6	(1)	F0pe	(6)									
44	T CrA	18 55.2	-37 06	11.8-13.6	(1)	F0e	(6)									
45	BD +40°4124	20 17.0	+41 03	10.6	(1)	B2e	(22)	-88	360	Em.(c)	X		Abs.:	296	19-Nov-81	42
46	BD +41°3731	20 20.8	+41 58	9.9	(1)	B2-B3	(1)	+ 4		Abs.				200	23-May-81	33
47	AS 442	20 44.1	+42 25	12	(14)	B8(e)	(14)	-23	170	Em.(d)			Abs.:	285	17-Nov-81	35
48	Lk Hα134	20 44.5	+43 25	12	(14)	B6-Ae	(14)	-75	200	Em.(s)				297	17-Nov-81	56
49	HD 200775	21 00.4	+67 47	7.4	(1)	B3e+s	(1)	-32	280	Em.(d)	X		Abs.	213	17-Nov-81	5
50	V645 Cyg	21 36.4	+49 47	13.6-14.8	(13)	O7e	(21)									
51	BD +65°1637	21 40.6	+65 39	11	(1)	B5e	(1)	-26	280	Em.(d)	X		Abs.:	207	16-Jun-81	45
52	Lk H 234	21 40.8	+65 39	11-13	(1)	B5-B7e	(22)	-25	140	Em.(c)				211	17-Jun-81	80
53	BD +46°3471	21 48.7	+46 46	10.1	(1)	A0e+s	(6)	-17	210	PCyg	X:	X		212	18-Jun-81	32
54	Lk Hα233	22 30.3	+40 08	14.5	(1)	A7e	(6)									
55	HD 216629	22 49.4	+61 36	9.0	(15)	B0-B8e	(15)	-10	340	Em.(s)			Abs.:	186	20-May-81	26
56	BLJ 71	23 01.1	+61 44	12	(15)	B0-B8e	(15)	-11	450	Em.(d)			Abs.:	217	18-Jun-81	79
57	MWC 1080	23 12.9	+60 18	13.0	(1)	eq	(6)	-63	220	PCyg		X	Abs.:	218	18-Jun-81	89
	Omega 1 Sco					B 1 V		+2.3								
	Pi And					B 5 V		+2.1								
	Tau And					B 8 V		+3.0								
	Mu And					A 5 V		+4.5								

References to table I.

(1) HERBIG, G. H. : 1960, *Astrophys. J. Suppl. Ser.* **4**, 337.
(2) HERBST, W. : 1975, *Astron. J.* **80**, 683.
(3) HERBIG, G. H. : 1980, private communication.
(4) ELIAS, J. H. : 1978, *Astrophys. J.* **224**, 857 & 453.
(5) PENSTON, M. V., ALLEN, D. A., LLOYD, C. : 1976, *Observatory* **96**, 22.
(6) HERBIG, G. H., RAO, K. N. : 1972, *Astrophys. J.* **174**, 401.
(7) COHEN, M., KUHI, L. V. : 1979, *Astrophys. J. Suppl. Ser.* **41**, 743.
(8) IRVINE, N. J. : 1975, *Publ. Astron. Soc. Pac.* **87**, 86.
(9) THÉ, P. S., TJIN A DJIE, H. R. E. : 1977, *IAU Coll.* **42**, 137.
(10) GLASS, I. S., ALLEN, D. A. : 1975, *Observatory* **95**, 27.
(11) POLIDAN, R. S. : *IAU Symp.* **70**, 414.
(12) APPENZELLER, I. : 1980, private communication.
(13) HUMPHREYS, R. M., MERRILL, K. M., BLACK, J. H. : 1980, *Astrophys. J. Lett.* **237**, L 17.
(14) HERBIG, G. H. : 1958, *Astrophys. J.* **128**, 259.
(15) ASSOUSA, G. E., HERBST, W., TURNER, K. C. : 1977, *Astrophys. J. Lett.* **218**, L 13.
(16) FINKENZELLER, U. : 1981, unpublished.
(17) RACINE, R. : 1968, *Astron. J.* **73**, 223.
(18) HENRY DRAPER CATALOG : 1922, Cambridge, Mass.
(19) REIPURTH, B. : 1983, *Astron. Astrophys.* **117**, 183.
(20) IRVINE, N. J., HOUK, N. : 1977, *Publ. Astron. Soc. Pac.* **89**, 347.
(21) COHEN, M. : 1977, *Astrophys. J.* **215**, 533.
(22) STROM, S. E., STROM, K. M., YOST, J., CARRASCO, L., GRASDALEN, G. : 1972, *Astrophys. J.* **173**, 353.
(23) This paper.

TABLE II. — *UBV and infrared data of Herbig Ae/Be stars.*

[1] #	[2] Star	[3] V̄	[4] ΔV	[5] N	[6] U−B	[7] B−V	[8] Ref.	[9] J	[10] H	[11] K	[12] L	[13] M	[14] Ref.	[15] Av	[16] IR Excess	[17] log Lmin/Lo	[18] log Lmax/Lo	[19] d[pc]
1	Lk Hα198	...	...	..	...	...		9.9	7.9	6.3	4.1	3.7	(23)	...	...	...	...	650
2	BD +61°154	10.71	0.37	4	−0.08	0.64	(1,2,4)	8.5	6.9	5.7	4.3	4.0	(23)	2.2	4.8	2.15	2.46	650
3	XY Per A+B	9.36	...	..	0.52	0.52	(2)	...	6.81	6.07	5.04	...	(24)	...	...	...	...	...
4	Elias 1	...	...	..	...	...		8.55	6.91	5.64	3.84		(31)	...	...	...	...	...
5	AB Aur	7.18	0.15	3	0.37	0.14	(2,4)	6.1	5.1	4.4	3.3	2.9	(23)	...	...	1.82	1.93	160
6	HK Ori	11.62	0.20	2	0.25	0.49	(1,3)	9.4	8.4	7.4	5.7	4.9	(23)	1.5	4.2	1.51	1.65	460
7	BD +9°880	...	...	..	...	...		...	...	...	...	...		...	...	...	...	...
8	T Ori	10.05	0.09	2	0.39	0.41	(7,13)	8.4	7.4	6.5	5.3	4.8	(23)	1.1	3.5	1.67	1.90	460
9	V380 Ori	10.32	0.30	6	−0.12	0.49	(1,2,3,5,6)	8.0	7.0	5.9	4.2	3.7	(23)	1.5	4.6	2.03	2.19	460
10	BF Ori	10.66	...	..	0.42	0.39	(10)	9.19	8.55	7.98	6.6	...	(26)	0.8	2.9	...	...	...
11	RR Tau	11.87	1.61	6	0.34	0.64	(1,4)	9.7	8.3	7.1	5.8	5.5	(23)	2.5	3.9	2.06	2.32	800
12	HD 37490	4.50	...	..	−0.81	−0.08	(2)	...	4.32	4.01	3.66		(27)	0.4	0.8	...	...	...
13	HD 250550	9.52	0.03	2	−0.26	−0.02	(4,13)	...	7.65	6.77	5.57	...	(24)	0.3	3.8	2.17	2.25	700
14	Lk Hα208	12.74	...	..	0.31	0.47	(3)	...	9.85	8.88	7.28	...	(24)	1.9	4.0	2.65	2.79	2000
15	MWC 137	12.05	...	..	−0.27	1.18	(12)	...	7.48	6.41	5.07	...	(13)	...	...	...	...	...
16	Lk Hα215	10.67	0.06	2	0.17	0.58	(3,14)	...	7.77	6.69	5.96	...	(24)	2.5	3.0	1.97	2.65	800
17	HD 259431	8.37	0.01	3	−0.54	0.27	(2,4,14)	...	6.56	5.62	4.58	...	(24)	1.4	3.3	2.76	3.16	800
18	R Mon	11.76	0.87	5	−0.19	0.64	(3,6)	9.5	7.8	5.9	3.1	...	(23)	2.8	7.0	3.10	3.17	800
19	L Hα25	12.93	0.56	4	−0.02	0.18	(4,8)	...	10.24	8.76	7.24	...	(28,10)	0.9	5.0	1.26	1.43	800
20	HD 52721	6.58	0.00	2	−0.76	0.06	(2,18)	6.29	6.23	6.10	5.96	...	(29)	0.8	0.6	3.46	3.82	1150
21	Lk Hα218	...	...	..	...	...		...	9.1	8.5	...	...	(24)	...	...	...	...	...
22	Z CMa	9.31	0.05	11	0.73	1.20	(4,33)	5.7	4.7	3.8	1.6	1.0	(23)	...	...	3.81	4.00	1150
23	Lk Hα220	...	...	..	...	...		...	...	...	...	...		...	...	...	...	...
24	HD 53367	6.98	0.00	2	−0.60*	0.44	(2,18)	5.76	5.48	5.18	4.81	...	(29)	2.3	0.9	3.57	4.01	1150
25	CoD −44°3318	10.61	0.05	7	...	...	(34)	8.47	7.24	5.99	4.40	3.85	(34)	...	...	...	...	...
26	HD 76534	8.04	...	..	−0.56	0.11	(17)	...	...	...	...	...		1.0	...	...	...	...
27	RCW 34	11.81	...	..	−0.12	0.92	(17)	...	...	...	...	...		...	...	...	...	...
28	RCW 36	...	...	..	...	...		...	...	...	...	...		...	...	...	...	...
29	Herbst 28	11.28	...	..	0.20	0.72	(17)	...	...	...	...	...		...	...	...	...	...
30	HD 97048	8.45	0.07	10	0.23	0.36	(9,13,19,20)	7.34	6.83	6.17	4.77	...	(29)	1.3	2.5	...	...	...
31	HR 5999	7.08	0.80	55	0.25	0.35	(16)	5.70	5.15	4.50	2.99	2.59	(16)	0.2	3.2	2.22	2.27	270
32	HD 150193	...	...	..	...	...		6.92	6.17	5.40	4.30	3.80	(30)	...	...	...	...	...
33	CoD −42°11721	...	...	..	...	...		...	...	...	...	...		...	...	...	...	...
34	KK Oph	10.32	...	..	0.45	0.67	(12)	...	6.68	5.43	4.03	...	(13,24)	1.6	4.3	...	...	...
35	HD 163296	6.84	...	..	0.06	0.07	(22)	...	5.22	4.49	3.59	...	(24)	0.3	3.8	...	...	...
36	Lk Hα118	11.13	...	..	−0.23	0.87	(12)	...	...	...	...	...		3.3	...	...	...	...
37	Lk Hα119	...	...	..	...	...		...	...	...	...	...		...	...	...	...	...
38	MWC 297	...	...	..	...	...		...	4.54	3.08	1.50	...	(24)	...	...	...	...	...
39	VV Ser	12.14	...	..	0.51	1.07	(12)	...	7.29	6.15	4.66	...	(24)	4.2	4.3	...	...	...
40	MWC 300	11.60	...	..	−0.15	1.01	(10)	...	8.17	5.98	3.31	...	(10,13)	...	...	...	...	...
41	AS 310	12.49	...	..	0.46	0.93	(12)	...	9.4	8.8	...	...	(31)	...	...	...	...	...
42	TY CrA	9.43	...	..	...	0.42	(10)	7.36	6.83	6.57	6.10	...	(26)	1.7	1.8	...	...	...
43	R CrA	10.74	...	..	0.10	0.56	(10)	7.22	5.07	3.43	1.78	...	(26)	1.9	7.2	1.84	1.90	150
44	T CrA	11.67	...	..	0.32	0.84	(10)	8.90	7.52	6.34	5.01	...	(26)	1.7	4.2	0.60	0.78	150
45	BD +40°4124	10.58	0.07	10	−0.36	0.78	(1,3,33)	8.0	6.9	5.7	4.2	3.8	(23)	3.0	4.0	2.58	3.12	1000
46	BD +41°3731	9.88	0.05	16	−0.50	0.10	(2,4)	9.9	9.8	9.6	...	...	(23)	1.1	...	2.07	2.54	1100
47	AS 442	...	...	..	...	...		...	7.75	6.46	5.16	4.2	(32,33)	...	...	...	...	...
48	Lk Hα134	...	...	..	...	...		...	8.66	7.99	6.79	...	(24)	...	...	...	...	...
49	HD 200775	7.38	0.05	5	−0.40	0.37	(2,4,33)	6.1	5.5	4.7	3.4	2.9	(23)	1.8	2.9	2.80	3.36	600
50	V645 Cyg	...	...	..	...	...		...	...	...	...	...		...	...	...	...	...
51	BD +65°1637	10.08	0.04	3	−0.36	0.40	(4)	9.0	8.7	8.6	8.0	7.5	(23)	1.8	0.8	1.98	2.68	1000
52	Lk Hα234	11.90	...	..	0.03	0.80	(2)	9.3	8.1	6.8	5.3	4.7	(23)	3.1	4.1	2.15	2.73	1000
53	BD +46°3471	10.12	0.07	14	0.17	0.42	(2,4,11,33)	8.6	7.7	6.7	5.1	...	(23)	1.7	3.7	1.56	2.73	1000
54	Lk Hα233	13.82	...	..	0.72	0.88	(3)	11.2	10.0	8.3	6.1	5.5	(23)	2.2	5.1	2.08	2.14	880
55	HD 216629	9.29	...	..	−0.19	0.72	(2)	...	...	...	...	...		3.1	...	...	...	...
56	BLJ 71	10.57	...	..	0.37	0.81	(21)	...	...	...	...	...		3.1	...	...	...	...
57	MWC 1080	11.71	0.26	2	0.22	1.29	(3,4)	7.4	6.0	4.7	2.9	2.4	(23)	...	...	2.40	...	500

References to table II.

(1) HERBIG, G. H. : 1960, *Astrophys. J. Suppl. Ser.* **4**, 337.
(2) RACINE, R. : 1968, *Astron. J.* **73**, 223.
(3) DIBAI, E. A. : 1969, *Astrophysics* **5**, 115.
(4) BREGER, M. : 1974, *Astrophys. J.* **188**, 53.
(5) MENDOZA, E. E. : 1966, *Astrophys. J.* **143**, 1010.
(6) MENDOZA, E. E. : 1968, *Astrophys. J.* **151**, 977.
(7) WALKER, M. F. : 1969, *Astrophys. J.* **155**, 447.
(8) WALKER, M. F. : 1956, *Astrophys. J. Suppl. Ser.* **2**, 365.
(9) HENIZE, K. G. : 1963, *Astron. J.* **68**, 280.
(10) HERBIG, G. H., RAO, N. K. : *Astrophys. J.* **174**, 401.
(11) WALKER, M. F. : 1959, *Astrophys. J.* **130**, 57.
(12) BASTIAN, U., MUNDT, R. : 1979, *Astron. Astrophys. Suppl. Ser.* **36**, 57.
(13) MUNDT, R., BASTIAN, U. : 1980, *Astron. Astrophys. Suppl. Ser.* **39**, 245.
(14) HERBST, W., MILLER, D. E., WARNER, J. W., HERZOG, A. : 1982, preprint.
(15) IRVINE, N. J., HOUK, N. : 1977, *Publ. Astron. Soc. Pac.* **89**, 347.
(16) THÉ, P. S. *et al.* : 1981, *Astron. Astrophys. Suppl. Ser.* **44**, 451.
(17) HERBST, W. : 1975, *Astron. J.* **80**, 212.
(18) HERBST, W., RACINE, R., WARNER, J. R. : 1978, *Astrophys. J.* **223**, 471.
(19) SCHWARTZ, R. D., NOAH, P. : 1978, *Astron. J.* **83**, 785.
(20) RYDGREN, A. E. : 1980, *Astron. J.* **85**, 444.
(21) ASSOUSA, G. E., HERBST, W., TURNER, K. C. : 1977, *Astrophys. J. Lett.* **218**, L 13.
(22) HAUPT, H. F., SCHROLL, A. : 1974, *Astron. Astrophys. Suppl. Ser.* **15**, 311.
(23) LORENZETTI, D., SARACENO, P., STRAFELLA, F. : 1983, *Astrophys. J.* **264**, 554.
(24) ALLEN, D. A. : 1973, *Mon. Not. R. Astron. Soc.* **161**, 145.
(25) PENSTON, M. V., ALLEN, D. A., LLOYD, C. : 1976, *Observatory* **96**, 22.
(26) GLASS, I. S., PENSTON, M. V. : 1974, *Mon. Not. R. Astron. Soc.* **167**, 237.
(27) GEHRZ, R. D., HACKWELL, J. A., JONES, T. W. : 1974, *Astrophys. J.* **191**, 675.
(28) STROM, S. E., STROM, K. M., YOST, J., CARRASCO, L., GRASDALEN, G. : 1972, *Astron. J.* **173**, 353.
(29) WHITTET, D. C. B., VON BREDA, I. G. : 1980, *Mon. Not. R. Astron. Soc.* **192**, 467.
(30) ELIAS, J. H. : 1978, *Astrophys. J.* **224**, 453.
(31) ALLEN, D. A. : 1974, *Mon. Not. R. Astron. Soc.* **168**, 1.
(32) ELIAS, J. H. : 1978, *Astrophys. J.* **224**, 857.
(33) HERBST, W., HOLTZMANN, J. A., PHELPS, B. E. : 1982, *Astron. J.* **97**, 1710.
(34) REIPURTH, B. : 1983, *Astron. Astrophys.* **117**, 183.

TABLE III. — *Stars with P Cygni line profiles at Hα and NaD :*
velocities and widths of various features in the line profiles shown in figure 1.

1	2	3	4	5	6	7
	Star	V_{max} (abs) Hα km/s	FWZI (abs) Hα km/s	V_{max} (abs) NaD km/s	FWZI (abs) NaD km/s	HWZI (em) NaD km/s
2	BD +61° 154	−350	220	−350: −200[a]	250: 150[a]	130: 120[a]
5	AB Aur	−400[b] −260	140[b] 100	−180[b] —	100[b] —	90[b] 100
22	Z CMa	−1000	900	−300 −500[a]	280 480[a]	—
35	HD 163296	−280	160	−220	120	200:
53	BD +46° 3471	−250	100	−150:	50:	110
57	MWC 1080	−400	180	−380 −350[a]	190 190[a]	120 140[a]

For HD 250550 the HWZI of the NaD emission, corresponding to column 7 , is 100 km/sec.

a) = from Figure 2   b) = from Felenbok et al. 1983

Notes to the individual columns:

#3   The maximum negative velocity of the P Cyg absorption of Hα is given in km/s.

#4   The total width of the P Cyg absorption of Hα at continuum level is given in km/s.

#5 , #6   are the values of NaD corresponding to column #3 and #4.

#7   The half width of the total NaD emission at continuum level is given in km/s .

TABLE IV. — *Previous $W_\lambda(H\alpha)$ measurements of Herbig Ae/Be stars* [Å].

	STAR	SPECTRAL TYPE	THIS WORK	COHEN AND KUHI (1979)	GARRISON AND ANDERSON (1977)	DIBAI (1969)	MEAN
2	BD +61°154	B8-B9eq	-34	-79	(-250)	-	-121
5	AB Aur	B9e	-22	-	-31	-	-27
6	HK Ori	A4ep	-45	-67	-	-	-56
8	T Ori	A3e	-13	-17	-	-	-16
9	V 380 Ori	A1e	-58	-90	-105	-70	-81
10:	BF Ori	A-Fpe	-13	-6	-	-	-10
11	RR Tau	A3-A5e	-50	-21	-29	-	-33
13	HD 250550	B9eq	-48	-43	-41	-	-44
14	Lk Hα208	B5-B9e	-5	-10	-	-	-8
16	Lk Hα215	B7-B8e	-17	-29	-	-30	-25
17	HD 259431	B6pe	-52	-60	-54	-	-55
19	L Hα25	B8pe	-44	-50	-	-	-47
21	Lk Hα218	B6e	-19	-25	-	-	-22
22	Z CMa	eq	+1	(-14)	-	-7	-7
23	Lk Hα220	B5e	-35	-53	-	-	-44
24:	HD 53367	B0IVe	-11	-	-19	-	-15
34	KK Oph	A5-A7e	-17	-26	-	-	-22
36	Lk Hα118	B5Vpe	-18	-22	-	-	-20
40:	MWC 300	eq	-78	-144	-	-	-111
45	BD +40°4124	B2e	-88	-	-68	-125	-94
49	HD 200775	B3Ve	-32	-	-38	-	-35
51	BD +65°1637	B5e	-26	-	-45	-	-36
52	Lk Hα 234	B5-B7e	-25	-41	-67	-	-44
53	BD +46°3471	AØ+s	-17	-	-18	-	-18
57	MWC 1080	eq	-63	-104	-59	-	-75

Following pages

FIGURE 1. — High resolution Hα and NaD (and He I $\lambda5876$) line profiles of 43 Herbig Ae/Be stars and Herbig Ae/Be star candidates ($\Delta V = 18$ km/s at FWHM, corresponding to a resolution of 0.4 Å at Hα). All spectra have been obtained with the Steward Observatory 90 inch-telescope echelle spectrograph using photographic plates behind a RCA image tube. The wavelength scale and velocity scale is in the earth rest frame. Accurate heliocentric radial velocity values (in km/s) are indicated at the profiles for a subset of 25 stars.   ➡
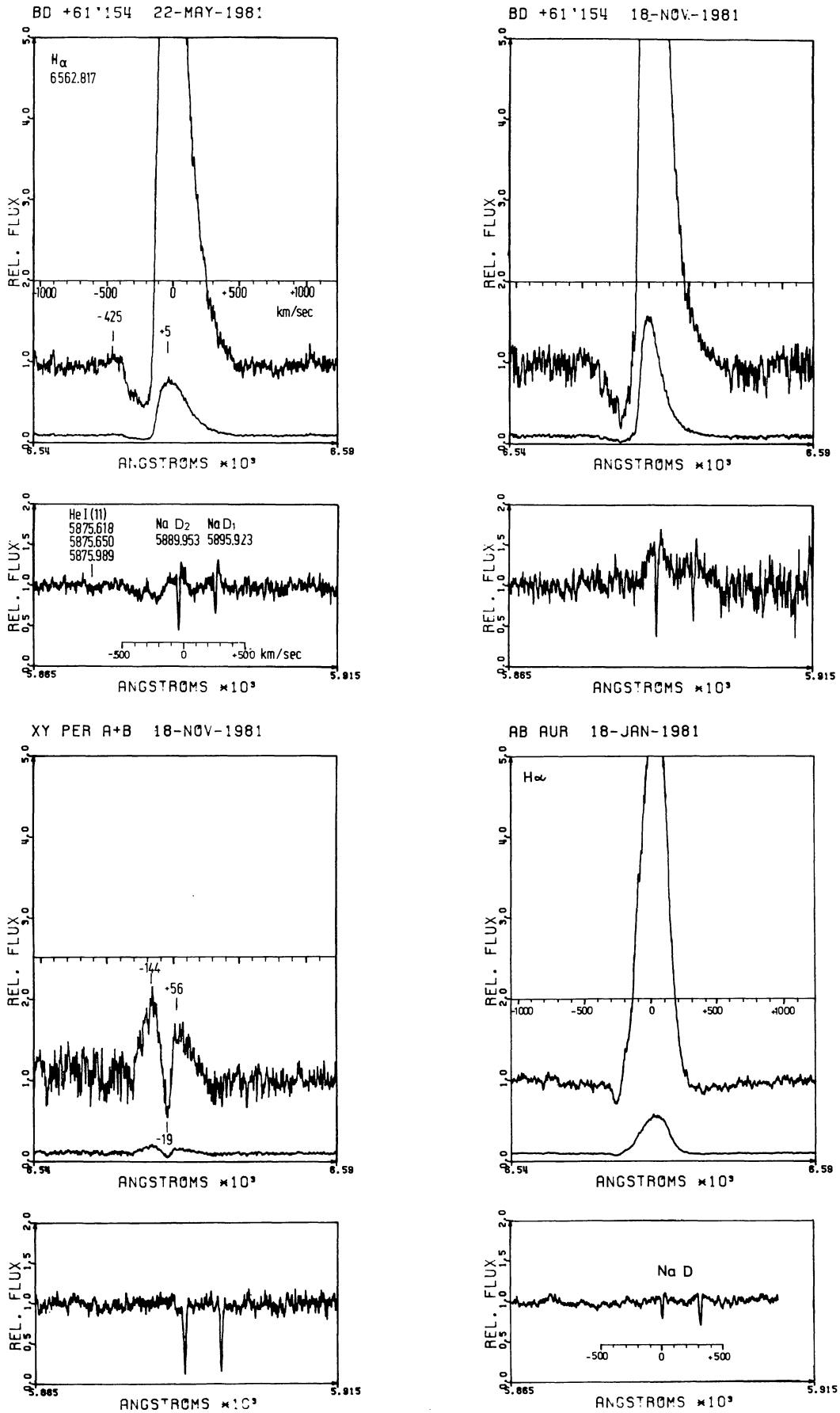
FIGURE 1
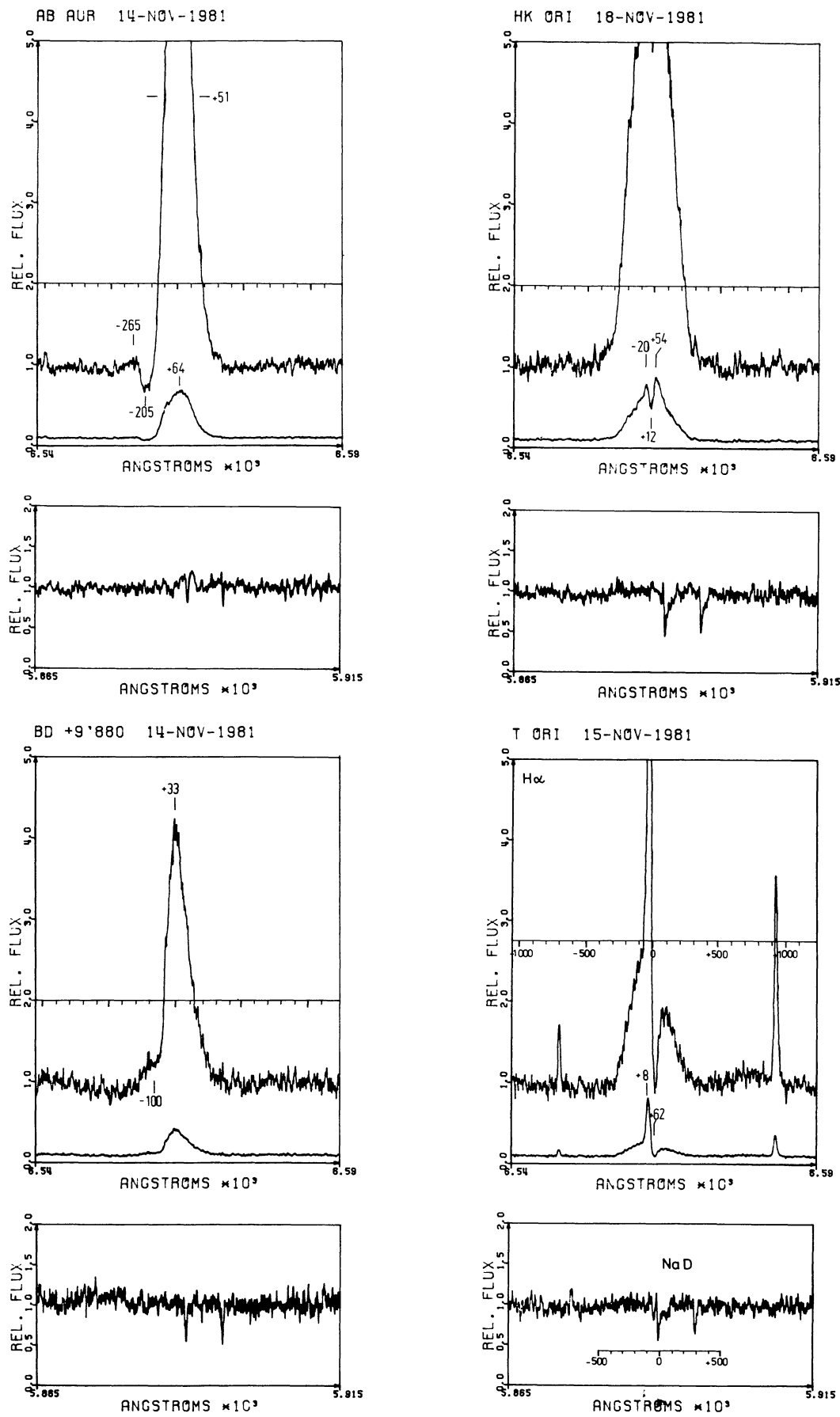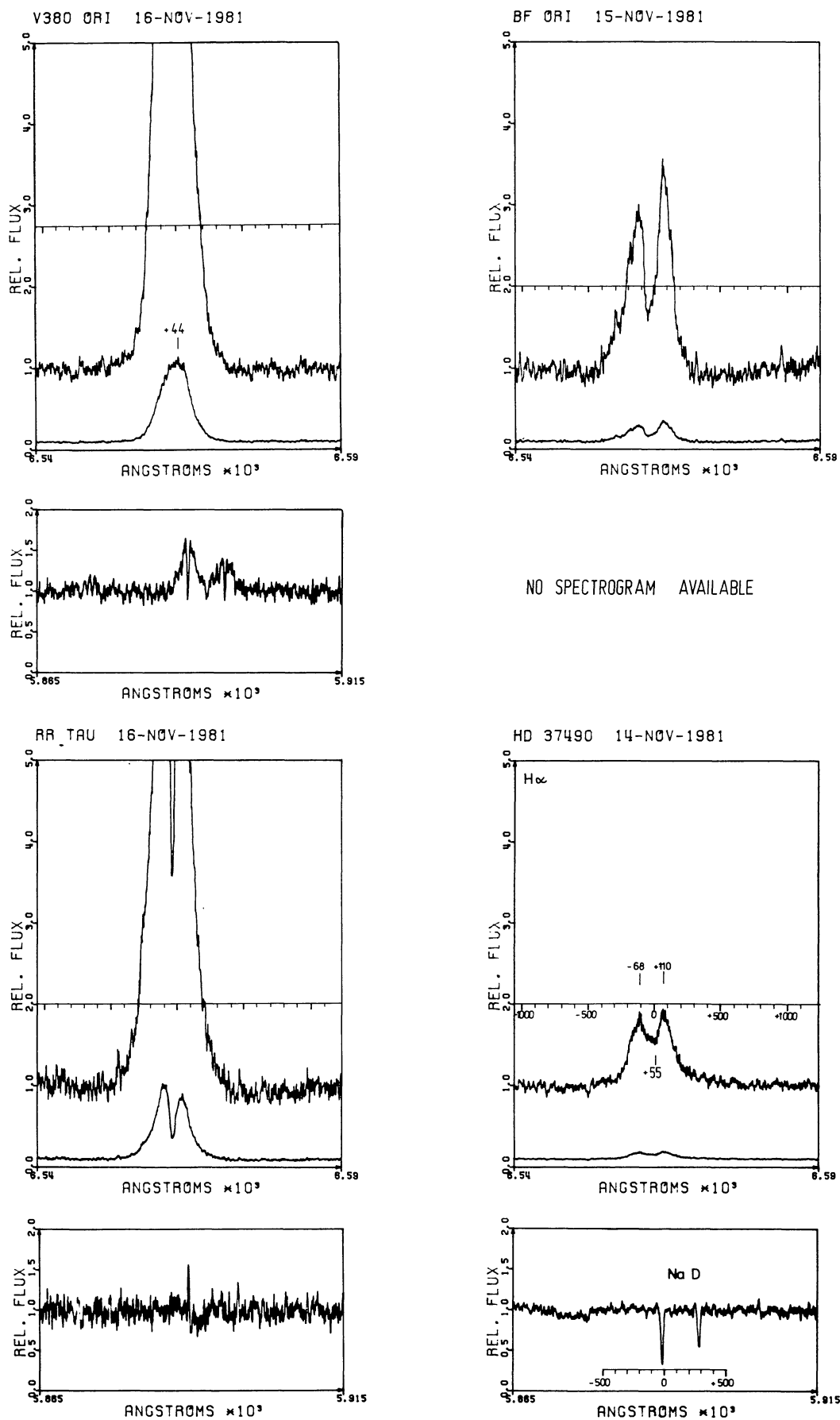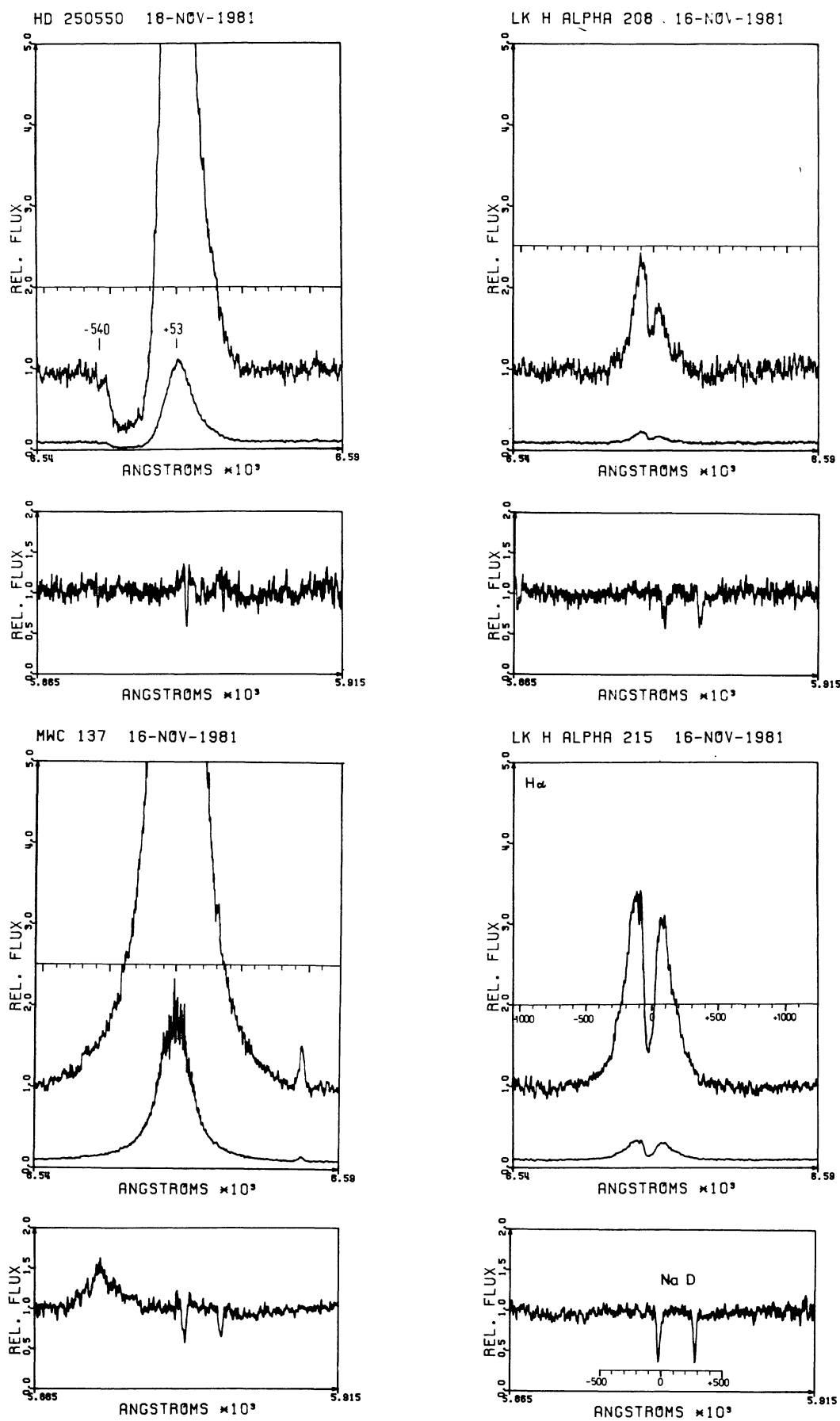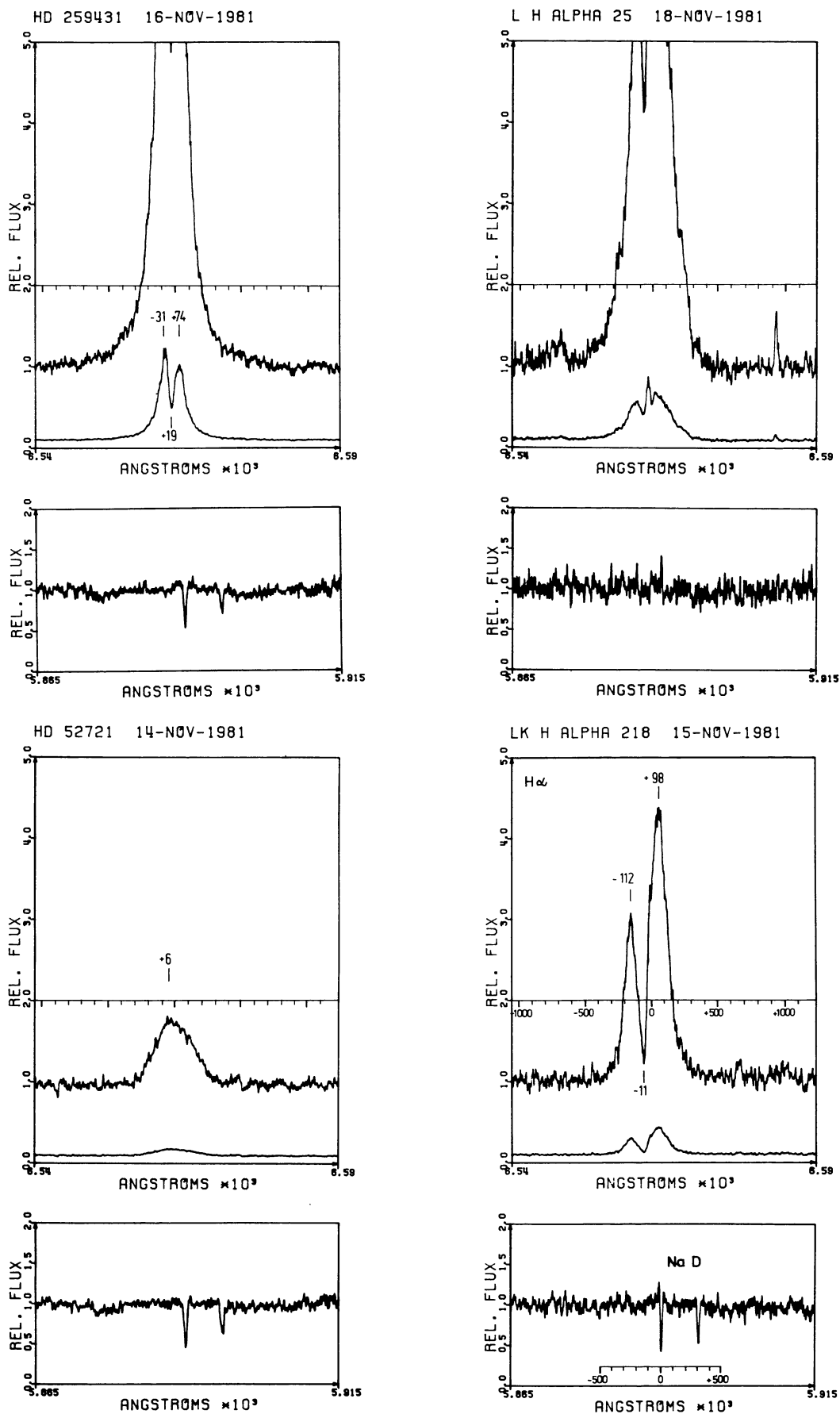
AB AUR   14-NOV-1981

HK ORI   18-NOV-1981

BD +9'880   14-NOV-1981

T ORI   15-NOV-1981

FIGURE 1 *(continued)*.

V380 ORI   16-NOV-1981

BF ORI   15-NOV-1981

REL. FLUX

+44

ANGSTROMS ×10³

REL. FLUX

ANGSTROMS ×10³

NO SPECTROGRAM   AVAILABLE

REL. FLUX

ANGSTROMS ×10³

RR TAU   16-NOV-1981

HD 37490   14-NOV-1981

Hα

REL. FLUX

-68 +110

+55

ANGSTROMS ×10³

REL. FLUX

ANGSTROMS ×10³

REL. FLUX

ANGSTROMS ×10³

Na D

REL. FLUX

ANGSTROMS ×10³

FIGURE 1 *(continued)*.

FIGURE 1 *(continued)*.

HD 259431   16-NOV-1981

L H ALPHA 25   18-NOV-1981

HD 52721   14-NOV-1981

LK H ALPHA 218   15-NOV-1981

FIGURE 1 (continued).

FIGURE 1 *(continued)*.

FIGURE 1 (continued).

FIGURE 1 *(continued)*.

FIGURE 1 *(continued).*

FIGURE 1 *(continued)*.

FIGURE 1 (continued).

HD 216629 20-MAY-1981

BLJ 71 18-JUN-1981

MWC 1080 18-JUN-1981

FIGURE 1 *(continued)*.

OMEGA 1 SCO   B 1 V

Hα

PI AND   B 5 V

HeI λ5876   NaD

TAU AND   B 8 V

MU AND   A 5 V
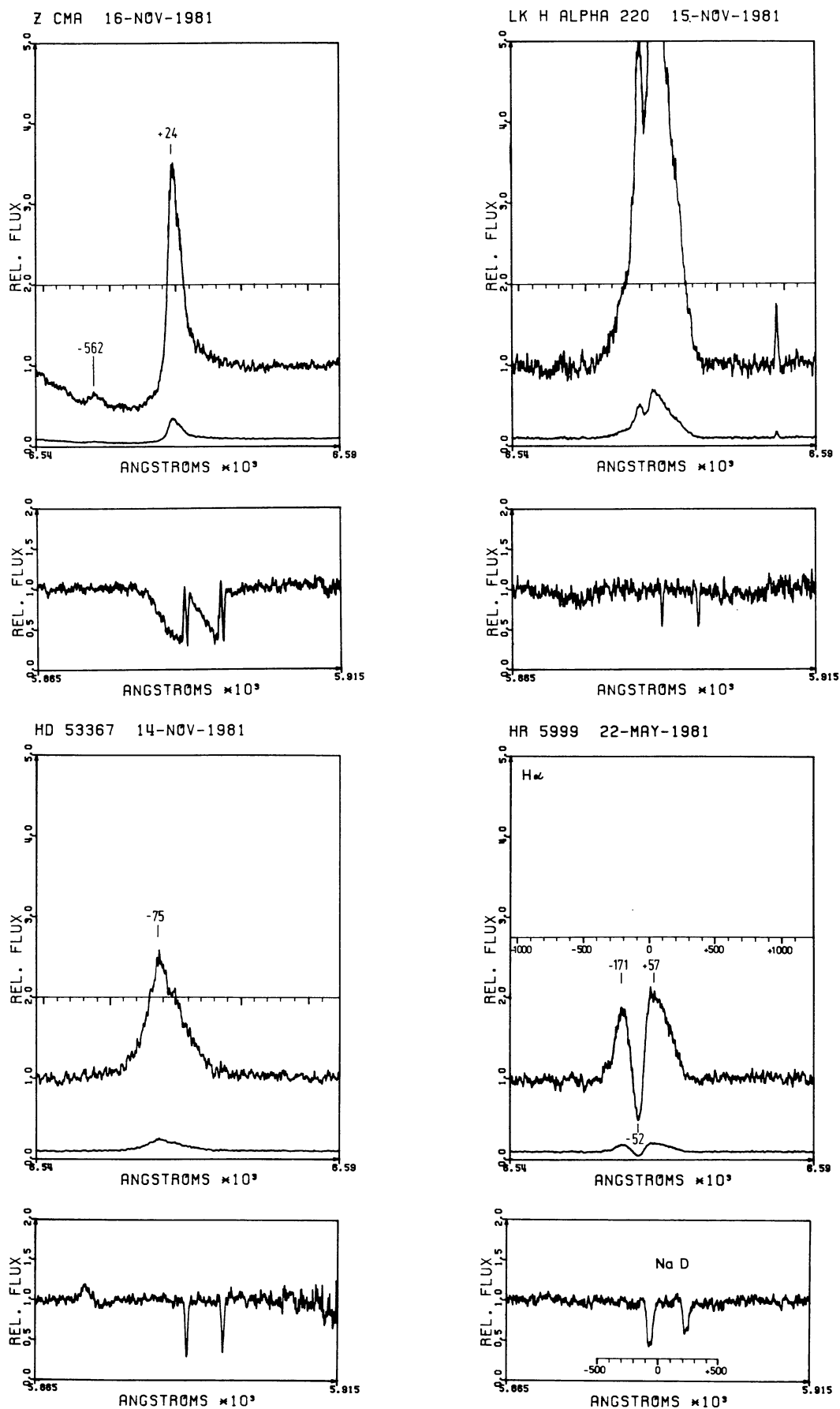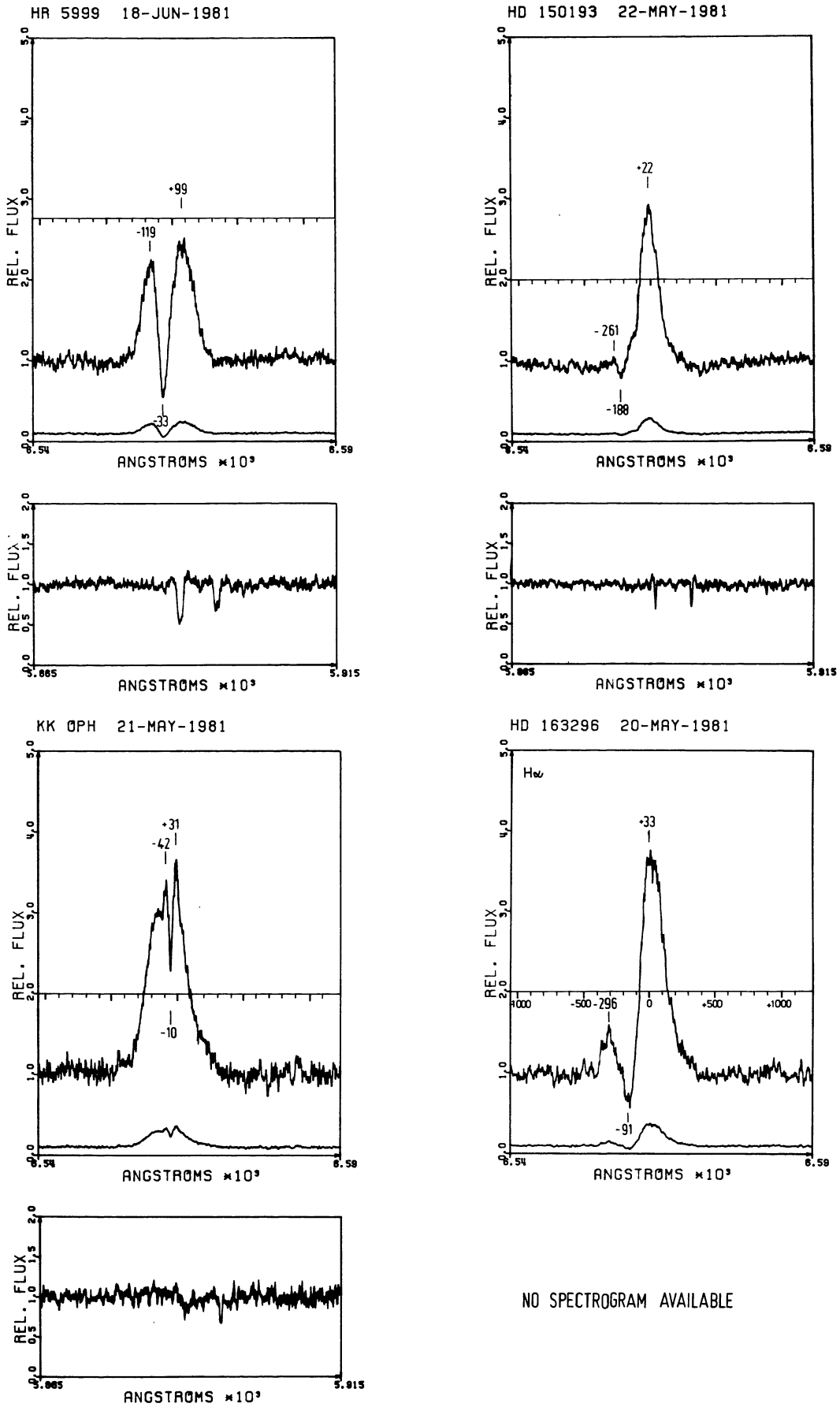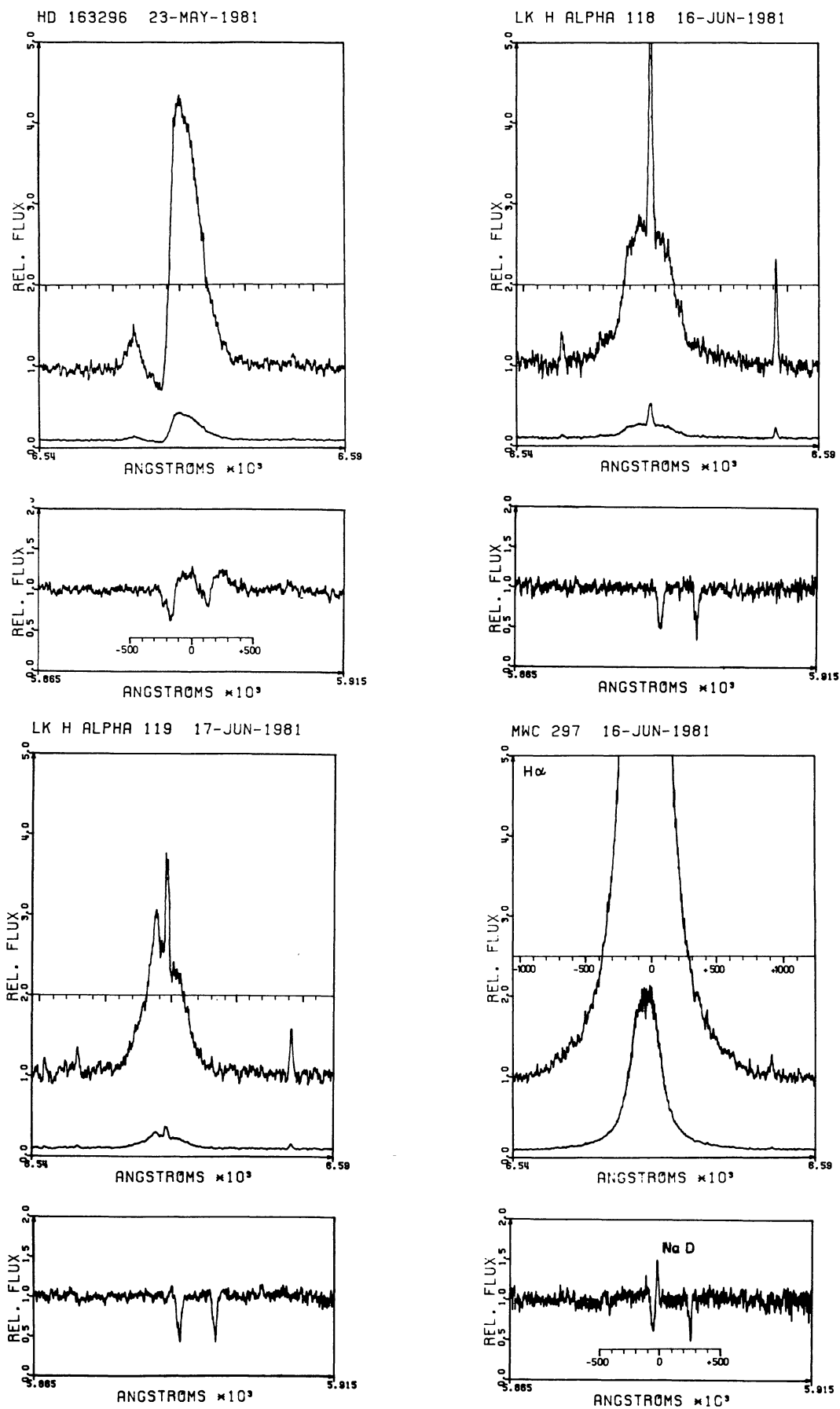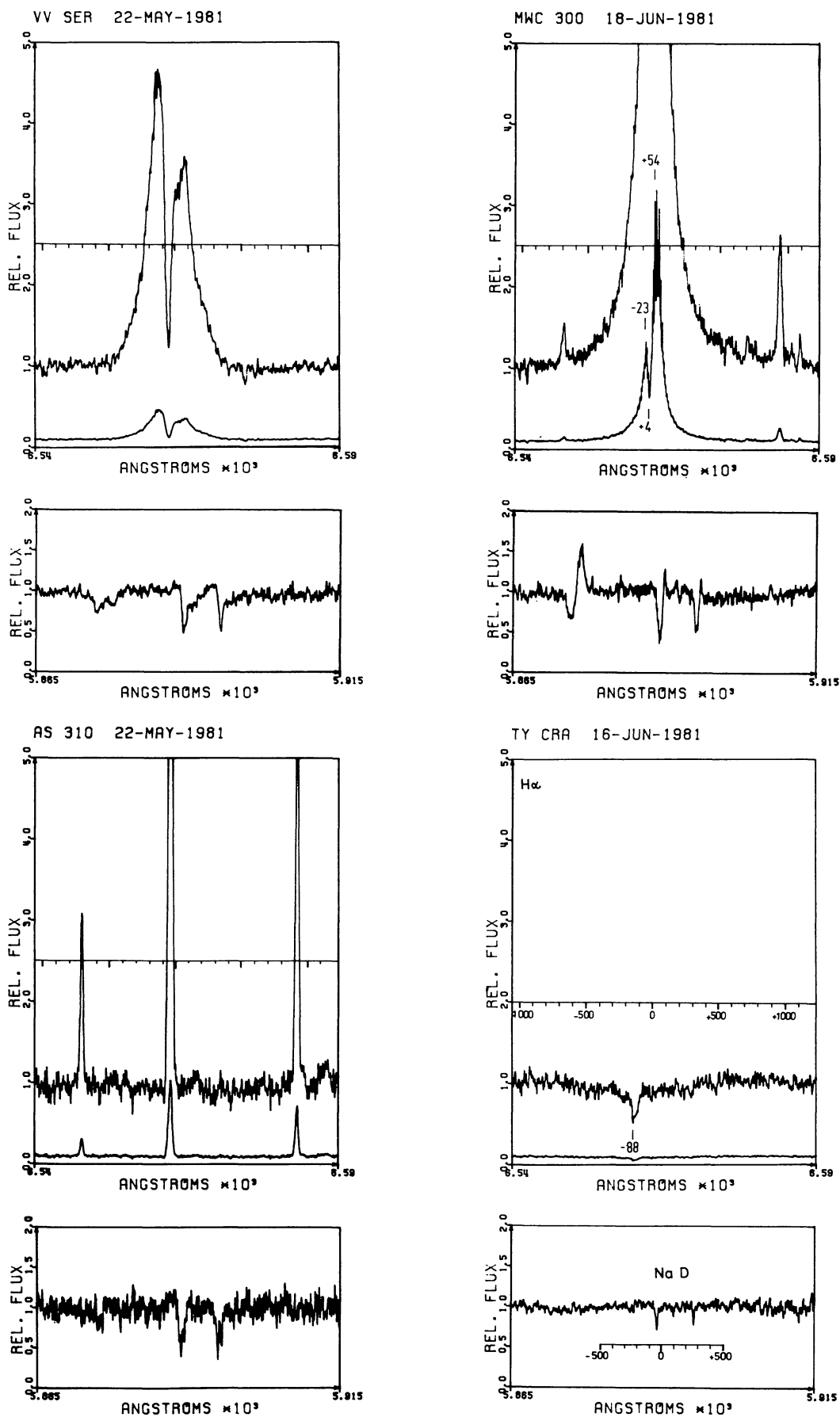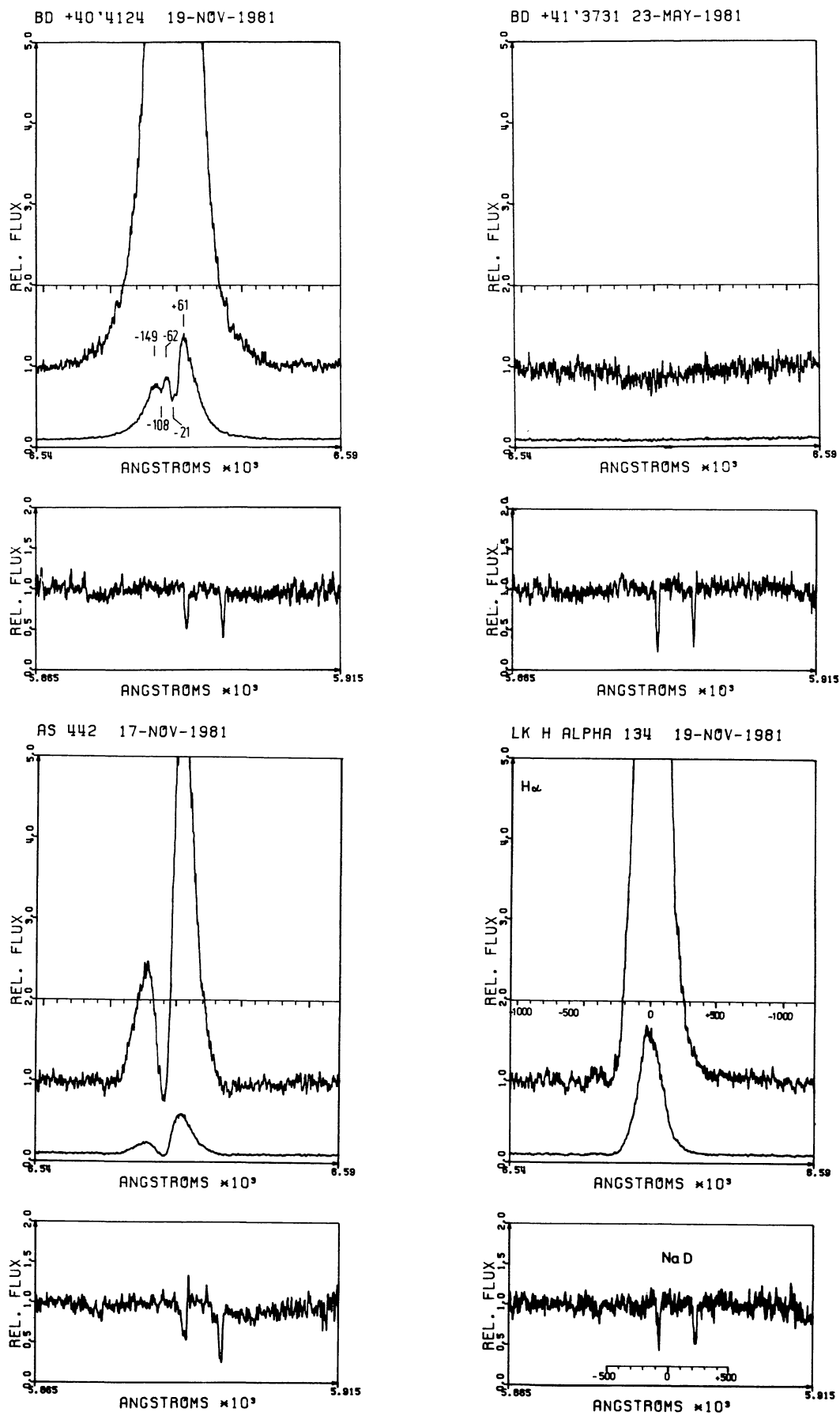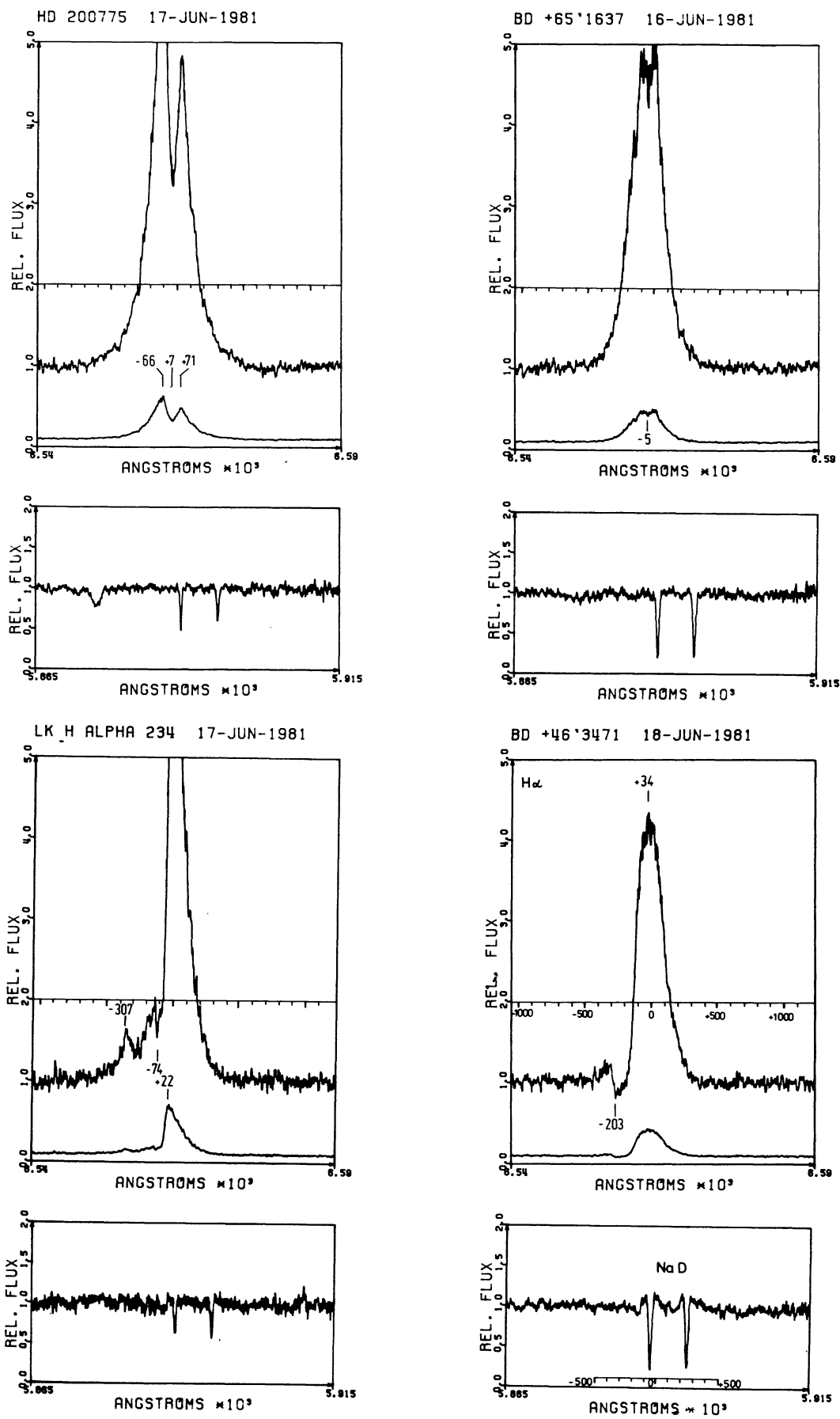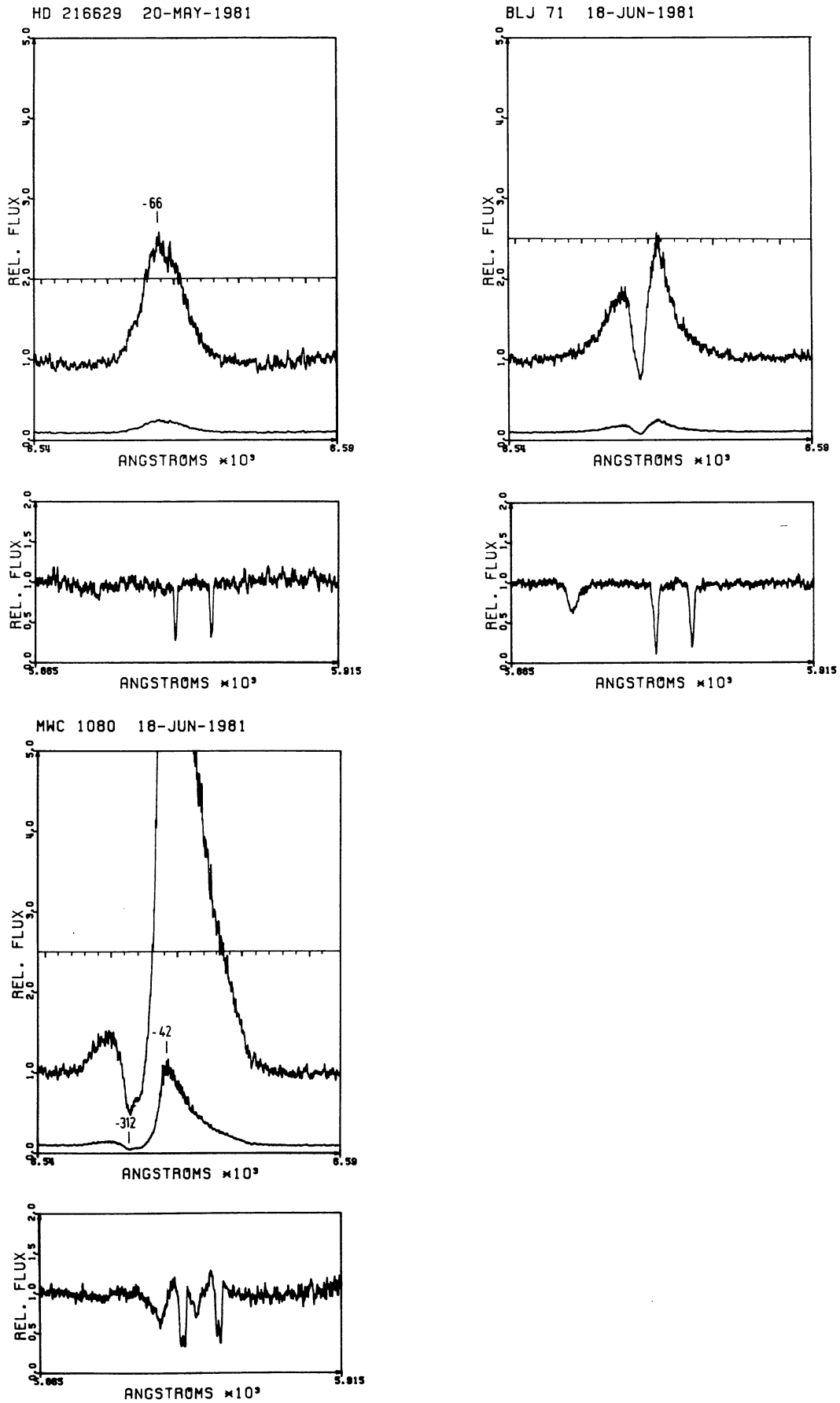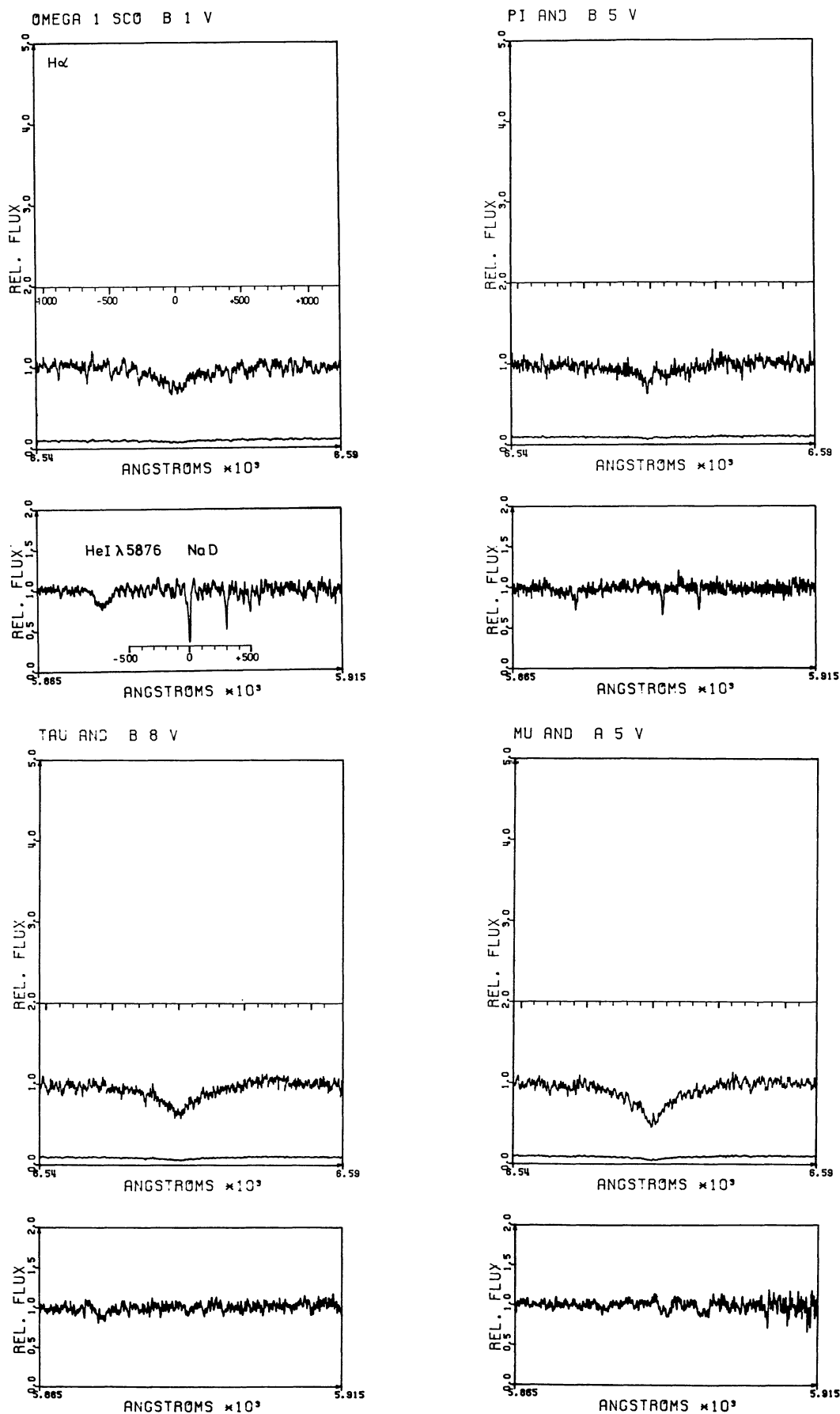
FIGURE 1 *(continued)*.
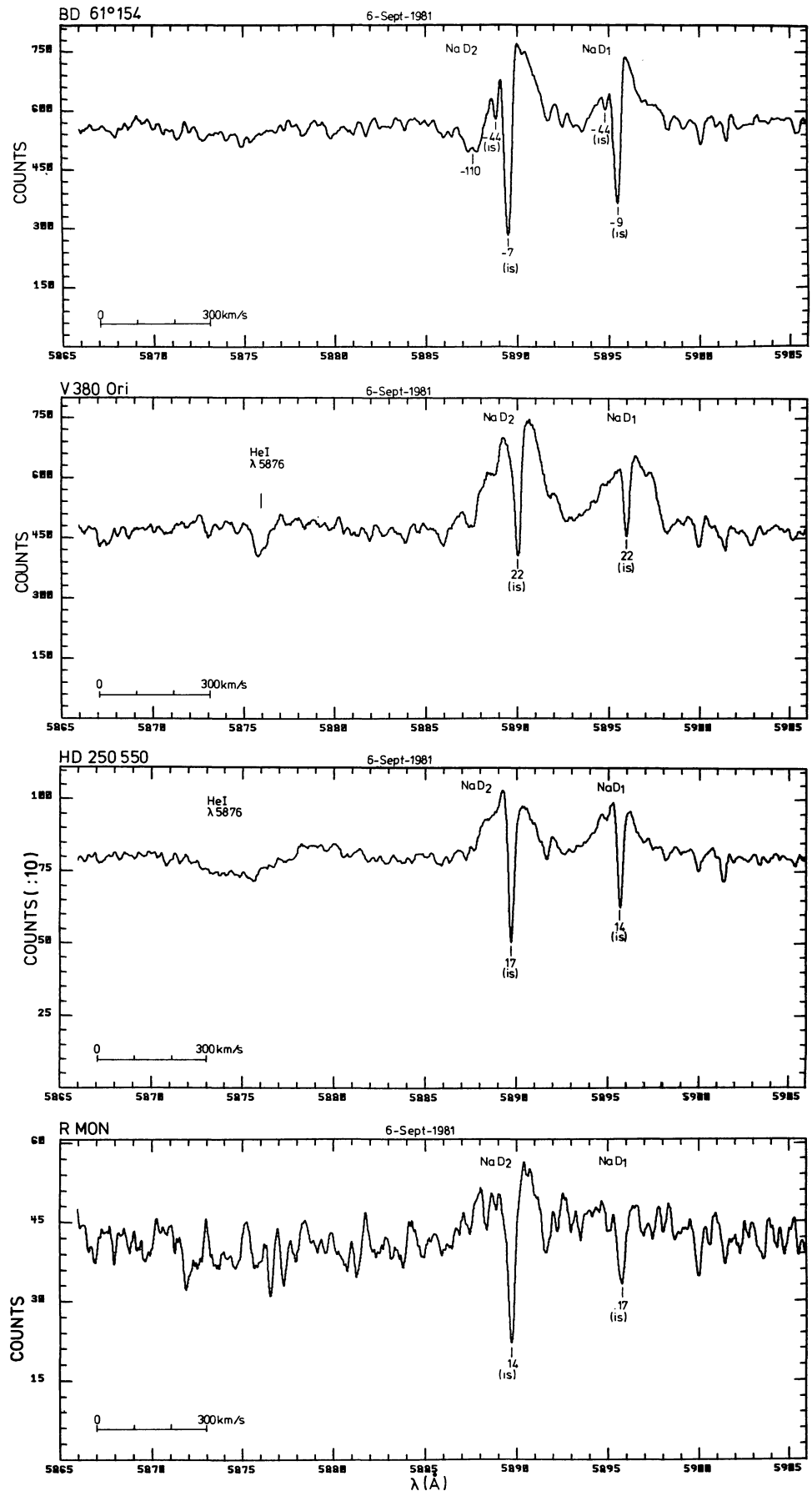
FIGURE 2. — High resolution NaD (and He I λ5876) line profiles of 8 Herbig Ae/Be stars ($\Delta V = 12$ km/s at FWHM, corresponding to a resolution of 0.24 Å). All spectra have been recorded with the Multiple Mirror Telescope echelle spectrograph using a photon-counting Reticon detector. The indicated numbers are heliocentric radial velocities in km/s. The interstellar absorption components are marked by « is ». The wavelength scale is in the earth rest frame. The ordinate is in counts/pixel (6 pixel ≈ 1 resolution element).
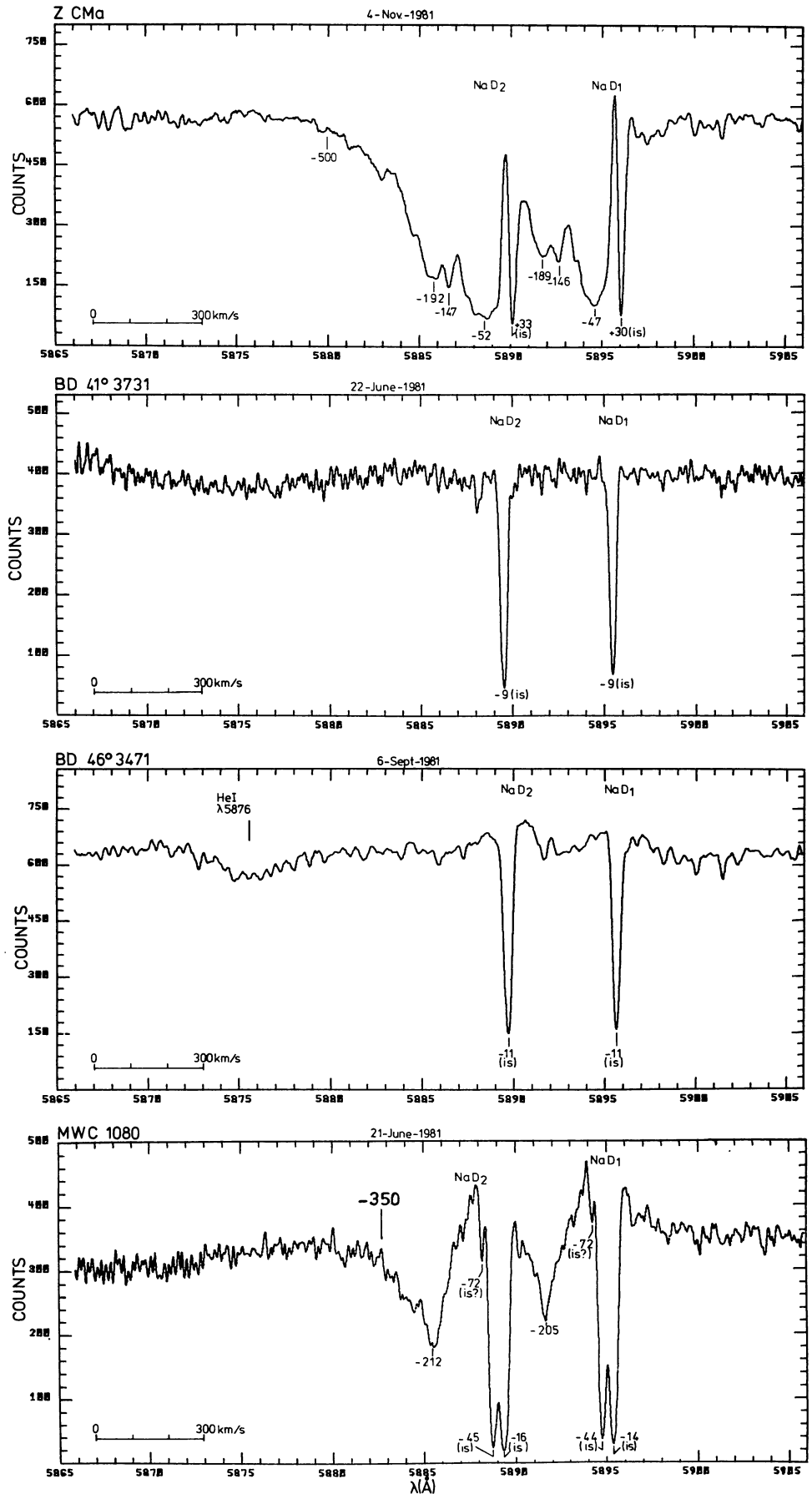
FIGURE 2 *(continued)*.
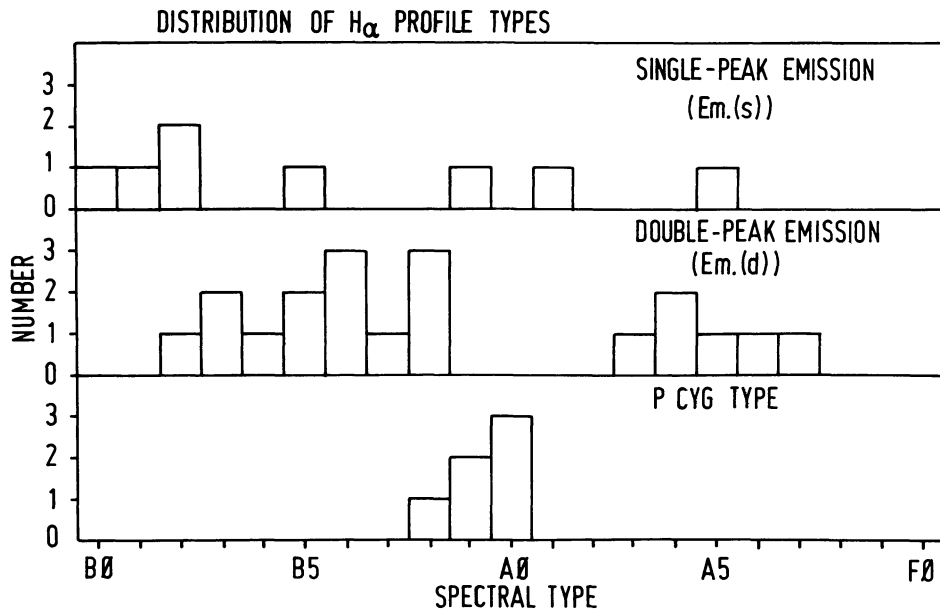
FIGURE 3. — Distribution of Herbig Ae/Be stars as a function of spectral type for the three different Hα line profile types.
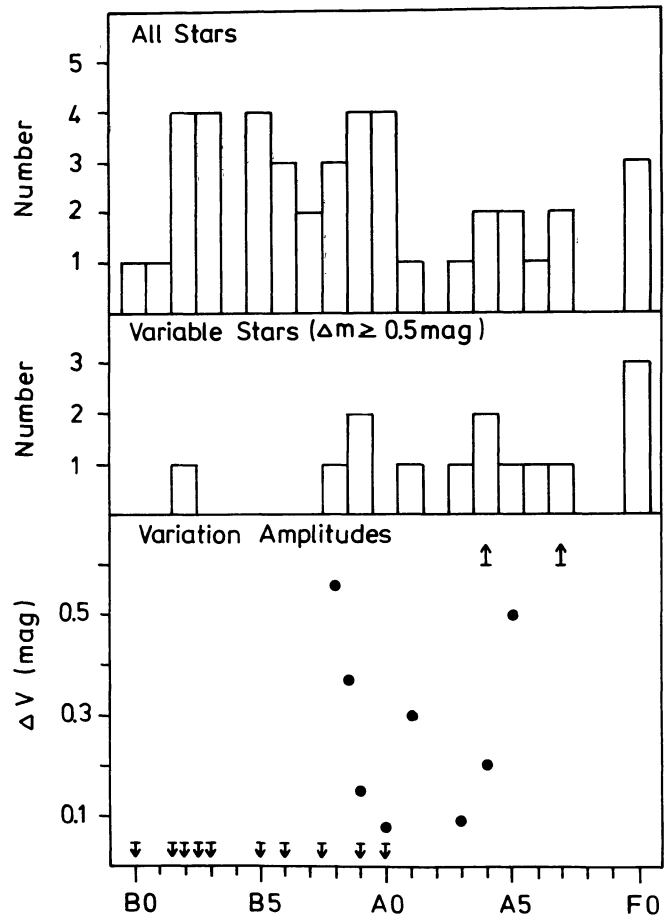

FIGURE 4. — Number of all known Herbig Ae/Be stars as a function of spectral type, compared to the distribution of variable HBeS and compared to the distribution of photoelectrically measured variation amplitudes.
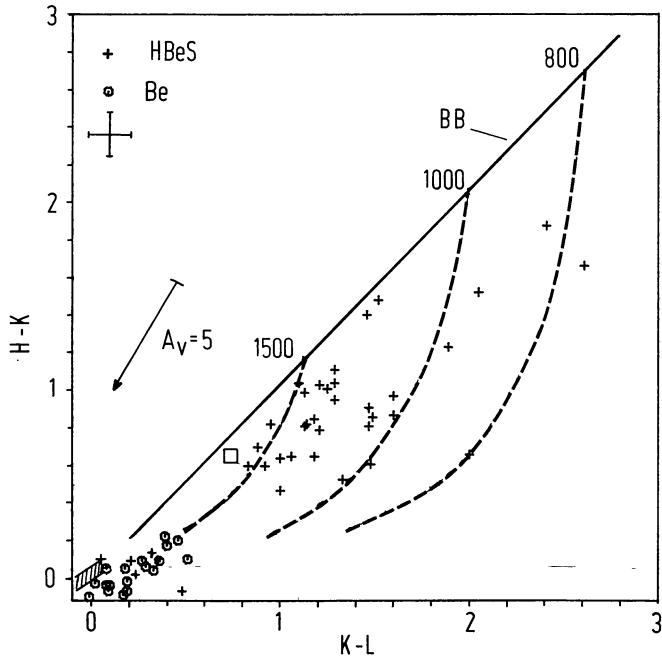
FIGURE 5. — Dereddened *H-K*, *K-L* two-color diagram of all Herbig Ae/Be stars for which colors are available from table II (crosses). For comparison a number of classical Be stars is plotted as well (open circles). Note the separation between these two stellar groups. The reddening vector shown corresponds to $A_V = 5$ mag. The typical error of the IR colors is indicated in the upper left hand corner. The main sequence from B0 to F0 is indicated as a hatched bar at the lower left hand corner. The square at $H\text{-}K = 0.67$ and $K\text{-}L = 0.74$ give the locus of the free-free, free-bound, and bound-bound emission from a optically thin hydrogen gas with $T_e = 10^4$ K. The three dashed curves are the locus of an A0 photosphere on which increasing amounts of thermal dust emission have been superimposed ($T = 800$, 1000, 1500 K).

FIGURE 6. — Hertzsprung-Russell diagram of Herbig Ae/Be stars. The crosses are lower limits of the bolometric luminosity (with no correction for interstellar extinction). The squares have been calculated by integrating over the extinction corrected 0.35 μ-5 μ energy distribution (assuming that all of the extinction is interstellar). The evolutionary tracks are from Iben (1965).